Terra Antartica
2004, **11**(1), 15-34

TERRA ANTARTICA
AN ANTARCTIC EARTH SCIENCE JOURNAL

High-Grade Crystalline Basement of the Northwestern Wilson Terrane at Oates Coast: New Petrological and Geochronological Data and Implications for Its Tectonometamorphic Evolution

U. SCHÜSSLER[1]*, F. HENJES-KUNST[2], F. TALARICO[3] & T. FLÖTTMANN[4]

[1]Institut für Mineralogie der Universität Würzburg, Am Hubland, D-97074 Würzburg - Germany
[2]Bundesanstalt für Geowissenschaften und Rohstoffe, Postfach 510153, D-30631 Hannover - Germany
[3]Dipartimento di Scienze della Terra, Via Laterina 8, I-53100 Siena - Italy
[4]CBU Exploration/Corporate New Ventures, Santos Ltd., 60 Edward Street,
Brisbane QLD 4000 (GPO Box 1010) - Australia

Received 1 October 2003; *accepted in revised form* 18 May 2004

Abstract – The high-grade basement of the northwestern Wilson Terrane at Oates Coast is subdivided into three roughly north-south trending zones on the basis of tectonic thrusting and differences in metamorphic petrology. New results of detailed petrological investigations show that metamorphic rocks of the central zone were formed in course of one single, clockwise directed P-T evolution including a medium-pressure and high-temperature granulite-facies stage at about 8 kbar and >800°C, a subsequent isothermal decompression and a final stage with retrograde formation of biotite + muscovite gneisses. In the eastern and western zones the majority of metamorphic rocks experienced clockwise oriented metamorphism at somewhat lower P-T conditions of about 4-5.5 kbar and 700–800°C. While some rocks in both zones did not reach the upper stability limit of muscovite + quartz, granulite-facies rocks detected in parts of the western zone were formed under P-T conditions similar to those of the central zone. New SHRIMP data support an age for the metamorphic peak of 496-500 Ma in the central zone (Henjes-Kunst et al., 2004). ^{40}Ar-^{39}Ar dating of amphiboles and micas indicate a general trend to younger ages from the west to the east of the basement complex, *i.e.* from 488–486 Ma to 472–469 Ma for amphiboles and from 484–482 Ma to 466 Ma for micas. This is explained by temporal differences in the retrograde metamorphic evolution of the three zones in the course of the late-Ross-orogenic thrust-related uplift of the basement complex, with the western zone being exhumed earlier than the eastern zone.

INTRODUCTION

Since 1988, the expeditions GANOVEX V and VII of the *Bundesanstalt für Geowissenschaften und Rohstoffe*, Hannover (Germany) and the joint German-Italian Antarctic Expedition 1999-2000 have visited Oates Coast (sometimes also called "Oates Land") west of northern Victoria Land at the Pacific end of the Transantarctic Mountains (Fig. 1a). During these expeditions, a systematic geological mapping and sampling was carried out for the first time in the Oates Coast area (*e.g.* Roland et al., 1996, 2001; Schüssler et al., 1998). In the frame of the GANOVEX V and VII expeditions in 1988/89 and 1992/93, respectively, it was recognized that the high-grade metamorphic basement of this area, forming the northern end of the Early Palaeozoic Ross Orogenic Wilson Terrane, is subdivided into three parallel orientated zones, commonly separated from each other and from adjacent low-grade metamorphic series by major thrusts (Flöttmann & Kleinschmidt,1991; 1993). Petrological and geochronological investigations concentrated on the central zone of the Oates Coast basement complex (Schüssler, 1996; Schüssler et al., 1999). Detailed results on the pressure-temperature-time evolution of the high-grade metamorphic rocks have now been obtained including data on abundant samples from the eastern and western zones of the basement complex. In particular, the joint German-Italian Antarctic Expedition 1999-2000 field investigations were focussed on the Lazarev Mountains in the western zone, where several locations were visited and sampled (Roland et al., 2000). This paper presents these new petrological and geochronological data and discusses their bearing on the tectonometamophic evolution of the high-grade Oates Coast basement complex.

GEOLOGICAL SETTING

The geology of northern Victoria Land and Oates Coast is comprised by three tectono-metamorphic terranes of Early Palaeozoic age, the easternmost Robertson Bay Terrane, the Bowers Terrane and the westernmost Wilson Terrane (Weaver et al., 1984;

**Corresponding author* (uli.schuessler@mail.uni-wuerzburg.de)

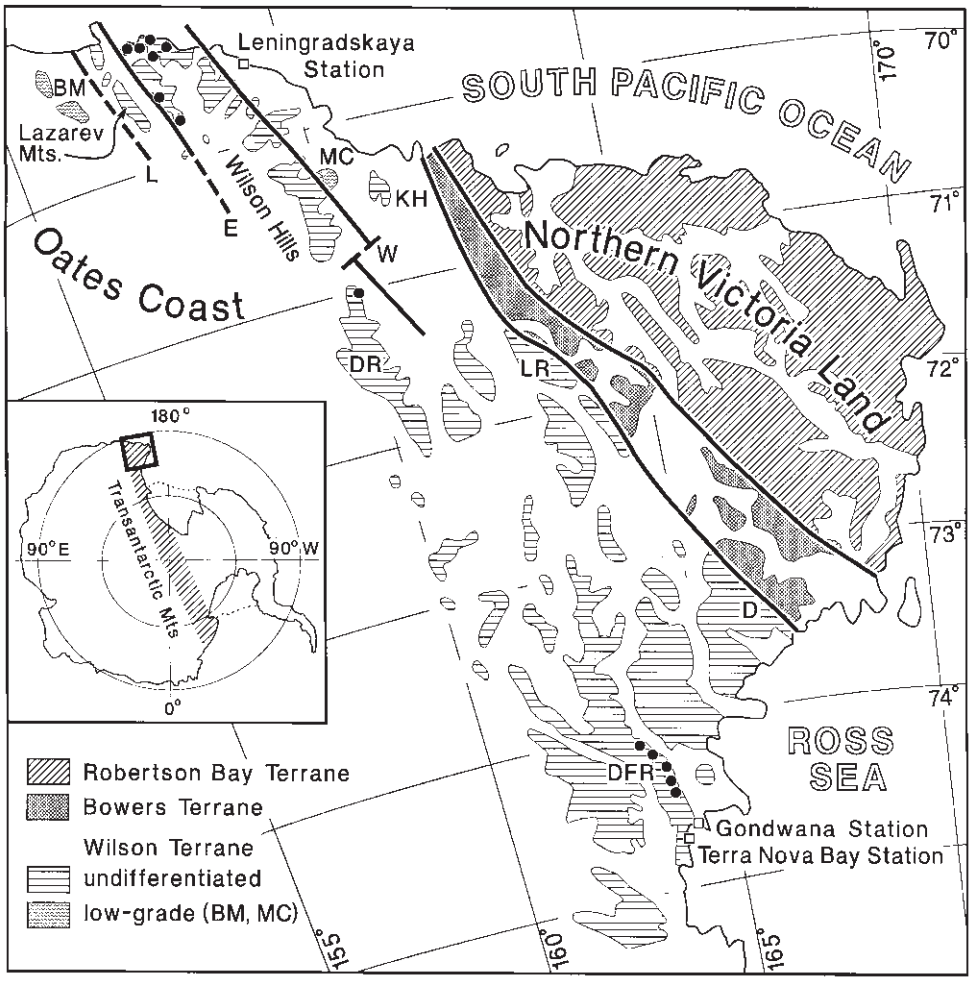

Fig. 1a – Geological sketch map of Oates Coast and northern Victoria Land. Cambro-Ordovician lithologies of the three tectonic terranes are undifferentiated except low-grade metasediments of McCain Bluff (MC) and Berg Mountains (BM). Post-Ordovician lithologies are omitted. Black dots denote occurrences of granulite-facies rocks. Thrusts: L, Lazarev Thrust; E, Exiles Thrust; W, Wilson Thrust. Mountain ranges: D, Dessent Ridge; DFR, Deep Freeze Range; DR, Daniels Range; KH, Kavrayskiy Hills; LR, Lanterman Range.

Fig. 1a). In the course of the late-Pan-African Ross Orogeny the Robertson Bay Terrane, a former flysch trough, and the Bowers Terrane, a former island arc, were accreted to the Wilson Terrane by plate convergence and craton-ward directed subduction processes (*e.g.* Gibson & Wright, 1985; Kleinschmidt & Tessensohn, 1987; Kleinschmidt et al., 1992; Dallmeyer & Wright, 1992; Matzer, 1995; Rocchi et al., 1998, the latter assuming an additional translation and rotation of a fore-arc span of the Wilson Terrane).

The Wilson Terrane, which is interpreted as the palaeo-Pacific active continental margin of the Antarctic craton affected by the Ross Orogeny, extends over about 600 km from the Ross Sea in the southeast to the Pacific coast in the northwest (Fig. 1a). Apart from various low- to medium-grade metamorphic rock suites, this terrane is characterized by an eclogite-bearing medium to ultrahigh P/medium to high T belt along its outboard margin to the north-easterly neighbouring Bowers Terrane (Dessent Ridge, Lanterman Range, see Fig. 1a) and a low to medium P/high T belt, in part granulite-bearing, at its southwestern inboard margin next to its suspected boundary with the East Antarctic Craton (Deep Freeze Range, Daniels Range, Oates Coast, see Fig. 1a) (Grew et al., 1984; Talarico 1990; Talarico & Castelli, 1994, 1995; Talarico et al., 1989, 1995; Di Vincenzo et al., 1997; Palmeri, 1997; Schüssler et al., 1999; Palmeri et al., 2003).

At the Oates Coast, the northern end of the low to medium P/high T metamorphic belt is exposed, geographically covering the Wilson Hills and the Lazarev Mountains (Fig. 1a). Due to the compressive tectonic regime during the Ross orogenic terrane accretion, the high-grade basement rocks of this area were detached and thrust along the Wilson Thrust to the east and along the Lazarev Thrust (also called western Exiles Thrust) to the west onto low-grade metasedimentary rocks of the Wilson Terrane, *e.g.* of McCain Bluff and the Berg Mountains, respectively (Figs. 1a, b; Flöttmann & Kleinschmidt, 1991, 1993; Roland et al., 1996, 2001; Schüssler et al., 1998), the latter having been intruded by the granites of the

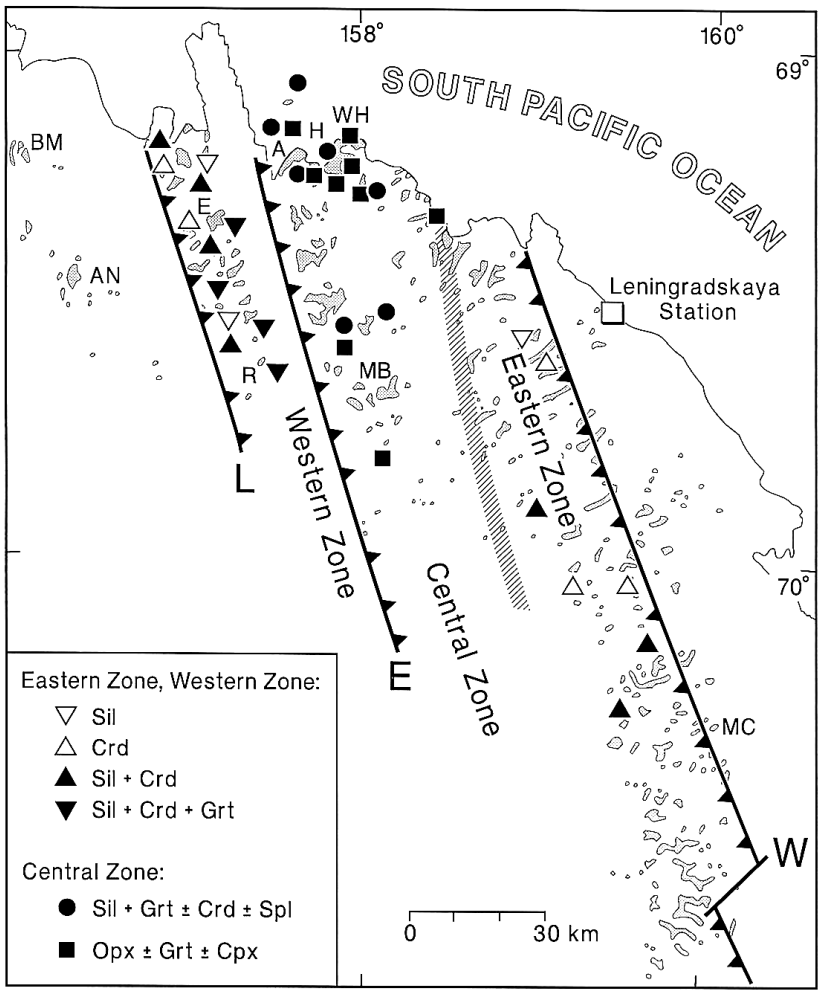

Fig. 1b – Regional distribution of critical phases within the metamorphic complex of the northern Wilson Terrane at Oates Coast. All mineral assemblages occur together with quartz, plagioclase, biotite and ± K-feldspar. Thrusts are labelled like in Fig. 1a. The hatched area indicates the transition between eastern and central zone. A, Mount Archer; AN, Archangel Nunataks; BM, Berg Mountains; E, Eld Peak; H, Harald Bay; MB, Mount Blowaway; MC, McCain Bluff; R, Rescue Nunatak; WH, Williamson Head.

Archangel Nunataks. Within the high-grade basement, thrust tectonics also led to the juxtaposition of zones with different metamorphic grades at the present level of exposure (Fig. 1b). The Exiles Thrust separates a western zone (*i.e.* the Lazarev Mountains) from a central zone east of the Matusevich Glacier. The boundary between the central zone and an eastern zone has not yet been analysed in detail, so that it is not clear wether it is a continuous transition or tectonic (Fig.1b).

The subdivision of the Oates Coast basement complex into an eastern, central and western zone was derived from petrological results (Schüssler, 1996; Schüssler et al., 1999). According to these investigations, the central zone has experienced granulite-facies metamorphism leading to mineral assemblages including sillimanite + garnet ± cordierite ± spinel and orthopyroxene ± garnet ± clinopyroxene. For the eastern and western zones, somewhat lower grade metamorphic conditions up to the formation of sillimanite + cordierite + K-feldspar are common. However, our new data show that parts of the western zone also reached granulite facies conditions.

Until now, only the central zone was petrologically and geochronologically investigated in detail. Using THERMOCALC (Powell & Holland 1994), P-T conditions were calculated for the formation of mineral assemblages of one sample and indicate a metamorphic evolution from an earlier medium-pressure granulite-facies metamorphism to a subsequent low-pressure granulite-facies to upper-amphibolite-facies metamorphism. The latter has taken place about 494 – 484 Ma ago during the Ross Orogeny, as determined by U-Pb dating of monazite from three samples (a slightly higher age of 500 – 496 Ma for the metamorphic peak was achieved by recent SHRIMP investigations on zircon from various samples of the central zone; Henjes-Kunst et al., 2004). However, it has remained unclear from these investigations whether the earlier medium-pressure granulite-facies assemblages belong to the same Early Palaeozoic event or are inherited from much older relics of the Precambrian Antarctic Craton. Cooling of the central zone from high-grade conditions was dated by Rb-Sr, K-Ar and Ar-Ar age determinations on micas from metamorphic rocks and an associated pegmatite, yielding ages varying between 476 and 470 Ma (Schüssler et al. 1999). Two Ar-Ar age spectra of 472 and 466 Ma were obtained from muscovites of two pegmatites in the eastern and central zone which intruded the basement with a

subsequent common cooling history (Henjes-Kunst, Flöttmann, Kleinschmidt, unpubl. results).

Based on the investigation of a larger number of samples, new petrological and thermobarometric data presented here provide more insight into the tectonometamorphic evolution of the central zone, especially highlighting the relations between the medium-pressure and the low-pressure granulite facies events. Furthermore, these investigations help to elucidate differences in the tectonometamorphic

Tab. 1 – Numbers, locations and description of mineral assemblages of important samples indicative for the metamorphic evolution or the age determination.

Eastern zone		
US-221	P.1420 wsw´ Mt. Shields, 70°12´S/159°44´E	Metatexite: Biotite + muscovite + plagioclase + quartz, biotite and muscovite retrograde, relics of sillimanite in muscovite
US-222	P.1250 wsw´ Mt. Shields, 70°12´S/159°38´E	Hornblende-gneiss: Ca-amphibole + plagioclase + quartz
US-227	P.1250 wsw´ Mt. Shields, 70°12´S/159°38´E	Leucosome in migmatite: biotite + sillimanite + cordierite + K-feldspar + plagioclase + quartz, sillimanite included in cordierite
US-231	Mt. Simmonds N-ridge 70°19´S/159°33´E	Gneiss: biotite + muscovite + sillimanite + plagioclase + quartz, prograde formation of sillimanite replacing muscovite
US-233	Mt. Simmonds N-ridge 70°19´S/159°33´E	Migmatite: biotite + sillimanite + cordierite + plagioclase + quartz + retrograde muscovite, pinitized cordierite containing relics of sillimanite
Central zone		
US-317	Eastern Exile Nunatak 69°55´S/158°06´E	Amphibolite: Ca-amphibole + plagioclase + quartz ± clinopyroxene
US-380	Thompson Peak E-ridge 69°24´S/157°44´E	Migmatite: garnet containing sillimanite in the rim area
US-390	Outcrop nw´ Stanwix Ridge 69°17´S/158°20´E	Migmatite: garnet + biotite + orthopyroxene + cordierite + plagioclase + quartz
MBA-1	P.1170 sw´ Mt. Blowaway 69°43´S/158°02´E	Ultramafic rock: olivine + orthopyroxene + spinel + Ca-amphibole + serpentine + phlogopite
US-408	Babuskin Island 69°06´S/157°36´E	Restite in diatexite: biotite + plagioclase + quartz + orthoamphibole, cummingtonite, Ca-amphibole completely replacing orthopyroxene
US-410	Babuskin Island 69°06´S/157°36´E	Restite in diatexite: garnet + biotite + cordierite + sillimanite + spinel + K-feldspar + plagioclase + quartz, sillimanite-inclusions in garnet, cordierite replacing garnet along the rims
US-445	Harald Bay, southern end 69°14´S/157°49´E	Migmatite: garnet + orthopyroxene + plagioclase + quartz + graphite + retrograde biotite, amphibole
US-447 ff	Harald Bay, southern end 69°14´S/157°49´E	Calc-silicate rocks: orthopyroxene ± biotite + clinopyroxene + plagioclase + quartz + amphiboles replacing orthopyroxene
HB-2	Harald Bay, southern end 69°14´S/157°49´E	Migmatite: garnet + biotite + cordierite + sillimanite + K-feldspar + plagioclase + quartz, sillimanite-inclusions in garnet, cordierite replacing garnet along the rims
HB-4	Harald Bay, southern end 69°14´S/157°49´E	Migmatite: garnet + cordierite + biotite + K-feldspar + plagioclase + quartz
HB-40	Harald Bay, southern end 69°14´S/157°49´E	Migmatite: orthopyroxene + biotite + plagioclase + quartz + amphiboles replacing orthopyroxene
US-473	Celestial Peak, NW-ridge 69°32´S/158°02´E	Migmatite: plagioclase + quartz + orthoamphibole, cummingtonite, Ca-amphibole completely replacing orthopyroxene
US-477	Celestial Peak, NW-ridge 69°32´S/158°02´E	Migmatite: garnet + cordierite + sillimanite + biotite + K-feldspar + plagioclase + quartz, sillimanite-inclusions in garnet and cordierite I, cordierite II replacing garnet along the rims
AP-2	Mt. Archer, N-ridge 69°12´S/157°39´E	Calc-silicate gneiss: othopyroxene + clinopyroxene + biotite + plagioclase + quartz
AP-7	Mt. Archer, N-ridge 69°12´S/157°39´E	Migmatic gneiss: garnet + orthopyroxene + biotite + plagioclase + quartz, orthopyroxene partly replaced by amphiboles
AP-12	Mt. Archer, N-ridge 69°12´S/157°39´E	Migmatite: garnet + biotite + spinel + sillimanite + K-feldspar + plagioclase + quartz + graphite, sillimanite and spinel included in garnet
US-501	Harald Bay, western end 69°13´S/157°45´E	Migmatite: garnet + biotite + sillimanite + cordierite + spinel + K-feldspar + plagioclase + quartz + graphite, cordierite, sillimanite and spinel included in garnet
US-503	Harald Bay, western end 69°13´S/157°45´E	Calc-silicate gneiss: orthopyroxene + clinopyroxene + plagioclase + quartz
WH1-11	Williamson Head, NE-ridge 69°11´S/158°02´E	Migmatite: garnet + orthopyroxene + biotite + plagioclase + quartz
US-507 ff	Williamson Head, S-ridge 69°14´S/158°01´E	Migmatite: orthopyroxene + biotite + plagioclase + quartz
US-509 ff	Williamson Head, S-ridge 69°14´S/158°01´E	Migmatite: garnet + orthopyroxene + biotite + K-feldspar + plagioclase + quartz + graphite
WH2-44	Williamson Head, S-ridge 69°14´S/158°01´E	Migmatite: garnet + biotite + sillimanite + cordierite + spinel + K-feldspar + plagioclase + quartz, sillimanite included in garnet
WH3-4	Williamson Head, central ridge, 69°12´S/157°58´E	Migmatite: garnet + orthopyroxene + biotite + cordierite + K-feldspar + plagioclase + quartz
WH4-3	Williamson Head, NW-ridge, 69°12´S/157°58´E	Migmatite: garnet + biotite + cordierite + sillimanite + spinel + K-feldspar + plagioclase + quartz, sillimanite included in garnet, garnet in part replaced by cordierite

evolution between the central zone and the eastern and western zones. Samples from the whole area have been studied for Ar-Ar age determinations in order to better constrain the ages of thrusting and the late Ross-orogenic exhumation history of the high-grade basement complex at the Oates Coast as a whole.

PETROGRAPHY AND MINERAL REACTIONS

The metamorphic basement at Oates Coast consists of extensive series of psammitic metasediments with local variations to more quartzitic or more pelitic compositions. Intercalations of layers or boudins of calc-silicate rocks are common, whereas amphibolitic layers are rare. Lenses of ultramafic rocks occur within the metasediments especially in the northern part of the central zone. During the 1999/2000 field campaign, such lenses have also been found along the eastern border of the western zone.

The clastic rocks underwent a more or less intensive migmatization. In the eastern and western zones, metatexites with low amounts of partial melt and stromatic migmatites with a clear subdivision into palaeosomes and neosomes (Mehnert 1968) and with formation of melanosomes and leucosomes prevail. In the central zone, migmatites are diatexites with high amounts of formerly molten material and in some cases with almost plutonic texture. Diatexites and agmatites occur also in the western zone, but are restricted to some limited outcrops (a few tens of meters wide) E of Mount Martyn along the eastern border of this zone.

Metasediments have mainly been derived from greywackes (Henjes-Kunst & Schüssler, 2003) and show a common assemblage consisting of biotite ± garnet + plagioclase ± K-feldspar + quartz. Few samples, more pelitic in composition, however, contain lighter or darker layers and schlieren in a cm or mm scale, with typical index mineral assemblages including cordierite, sillimanite, garnet, spinel or orthopyroxene. Individual samples with indicative assemblages are listed in table 1.

EASTERN AND WESTERN ZONES

In one sample from the eastern zone (US-231 Mt. Simmonds) and four samples from the western zone (US-378 and –379 highpoint 740 north of Rescue Nunatak, MS-3487 Burnside Ridge, 23.1T13 Drury Nunatak), assemblages of sillimanite + biotite + plagioclase ± muscovite + quartz occur, with

Tab. 1 – Continued.

Western zone		
27.1T8	Rescue Nunatak 69°37´S/157°26´E	Migmatite: Garnet + biotite + cordierite + sillimanite + plagioclase + quartz, sillimanite included in garnet, cordierite rims around garnet
US-378	P.740 N of Rescue Nunatak 69°31´S/157°25´E	Gneiss: biotite + sillimanite + muscovite + plagioclase + quartz, all in contact assemblage
US-379	P.740 N of Rescue Nunatak 69°31´S/157°25´E	Gneiss: garnet + biotite + sillimanite + muscovite + plagioclase + quartz, beginning reaction between sillimanite and biotite
MS-3478	P.740 N of Rescue Nunatak 69°31´S/157°25´E	Gneiss: garnet + biotite + sillimanite + cordierite + muscovite + plagioclase + quartz, reaction between sillimanite and biotite forms first cordierite
28.1T8	P.740 N of Rescue Nunatak 69°31´S/157°25´E	Migmatite: garnet + biotite + sillimanite + cordierite + K-feldspar + plagioclase + quartz, sillimanite included in garnet and cordierite, cordierite around garnet
28.1T13	Between P.740 and Mt. Martyn, 69°28´S/157°18´E	Gneiss: garnet + biotite + sillimanite + cordierite + K-feldspar + plagioclase + quartz, sillimanite included in cordierite, locally in contact to biotite
29.1T3	Nunatak SE´ Mt. Martyn 69°26´S/157°17´E	Sillimanite inclusions in cordierite, cordierite rim around garnet
MS-3475	Mt. Martyn, SW-ridge 69°24´S/157°11´E	Gneiss: biotite + sillimanite + cordierite + K-feldspar + plagioclase + quartz, sillimanite included in cordierite, locally in contact to biotite
31.1T8	Mt. Martyn, N-ridge 69°23´S/157°11´E	Sillimanite inclusions in cordierite, cordierite replaces garnet along the rims
26.1T17	Eld Peak, E-ridge 69°21´S/157°11´E	Sillimanite inclusions in cordierite, discontinuous cordierite rim around garnet
MS-3486	Reynolds Peak 69°15´S/157°02´E	Gneiss: garnet + biotite + sillimanite + cordierite + plagioclase + quartz, sillimanite included in cordierite
US-437	Ridge between Coombes Ridge and Reynolds Peak, 69°12´S/157°04´E	Gneiss: biotite + sillimanite + cordierite + K-feldspar + plagioclase + quartz, sillimanite included in cordierite, locally in contact to biotite
MS-3487 ff	Burnside Ridge, S-ridge 69°13´S/157°12´E	Metatexite: biotite + sillimanite + muscovite + K-feldspar + plagioclase + quartz, sillimanite in contact with biotite and adjacent quartz
MS-3490	Burnside Ridge, S-ridge 69°13´S/157°12´E	Amphibole-gabbro: Ca-amphibole + plagioclase
23.1T13	Drury Nunatak 69°14´S/156°57´E	Gneiss: sillimanite + biotit + plagioclase + quartz, sillimanite in contact with biotite
US-405	Drury Nunatak 69°14´S/156°57´E	Migmatite: cordierite + biotite + K-feldspar + plagioclase + quartz
MS-3495	Ridge N of Drury Nunatak 69°11´S/156°50´E	Gneiss: cordierite + biotite + sillimanite + plagioclase + quartz, sillimanite includes in cordierite

coexisting sillimanite + biotite in the presence of quartz, with coexisting primary muscovite + quartz, or with sillimanite just replacing muscovite or in a beginning reaction with biotite. These samples represent the lowest metamorphic grade in both zones, when the following reactions have still not or just started:

(1) muscovite + quartz
= silimanite + K-feldspar + V/melt
(2) sillimanite + biotite + quartz + V
= cordierite + muscovite
(3) sillimanite + biotite + quartz =
cordierite + K-feldspar + V/melt

(Chatterjee & Johannes, 1974; Holdaway & Lee, 1977; Loomis, 1976; Xu et al., 1994)

More common are assemblages with sillimanite + cordierite + biotite ± K-feldspar ± garnet + plagioclase + quartz, in which spindle-shaped cordierite is surrounded by biotite and includes relics of fibrolitic sillimanite, indicating that reaction (3) has taken place. K-feldspar is not always present (probably as a consequence of K^+ being removed by the fluid phase). Garnet, if present, commonly does not include sillimanite. Exceptions to this are two samples of the western zone (27.1T8 Rescue Nunatak and 28.1T13 small Nunatak north of Rescue Nunatak), where relics of sillimanite were observed within cordierite and garnet, indicative for the granulite-facies reaction

(4) sillimanite + biotite + quartz
= cordierite + garnet + K-feldspar + V/melt

(for example Holdaway & Lee, 1977). The replacement of garnet by cordierite along the rims, observed in these two and some further samples, is due to reaction (6)(see below).

Parts of these samples are strongly affected by a retrogressive overprint with more or less complete replacement of cordierite by a second generation of muscovite, but with relics of sillimanite still remaining in the centres of the pseudomorphs.

CENTRAL ZONE

Assemblages consisting of sillimanite + garnet + cordierite ± spinel + biotite + K-feldspar + plagioclase + quartz are widespread. Sillimanite is almost always included in garnet, commonly in the rim regions, rarely it is present in the garnet cores. In some samples, sillimanite is also included in cordierite. Both garnet and cordierite are therefore inferred to have formed in the course of reaction (4). Green spinel which often occurs in association with garnet and/or cordierite may have formed by reaction

(5) sillimanite + biotite + quartz
= cordierite + spinel + K-feldspar (+ ilmenite) + V/melt

(Loomis, 1976; Grant, 1985; Schubert & Olesch, 1989, Hensen & Harley, 1990). In sillimanite-free assemblages consisting of cordierite + garnet + biotite ± plagioclase ± quartz, euhedral cordierite is sometimes in textural equilibrium with euhedral garnet, showing straight common grain boundaries (sample HB-4, Tab. 1).

Garnet with sillimanite inclusions is often replaced by a second generation of cordierite. The replacement starts from rims or cracks of the garnet and is consistent with the reaction

(6) garnet + sillimanite + quartz + V = cordierite

(for example Holdaway & Lee, 1977). Sometimes the transformation into cordierite is complete. In extreme cases, only a small garnet remains enclosed in large cordierite blasts.

Typical for the central zone are rocks with orthopyroxene-bearing parageneses, the simplest of which is orthopyroxene ± biotite + plagioclase + quartz. In addition, clinopyroxene, garnet, cordierite and K-feldspar may occur. If garnet is present, this mineral is sometimes in textural equilibrium with orthopyroxene. More commonly, however, orthopyroxene is more or less decomposed retrogressively and replaced by symplectites of biotite + quartz or by amphiboles, often intergrowths of orthoamphibole + cummingtonite + Ca-amphibole. In many samples, the former presence of orthopyroxene is still indicated by pseudomorphs consisting of such amphibole intergrowths. If present, garnet is also replaced at its rims by fine-grained aggregates of sheet silicates (micas, chlorite).

In few samples, euhedral garnet without sillimanite inclusions shows inclusions of biotite oriented in the same direction of biotite of the matrix rock. This garnet is interpreted as having formed during a late stage of metamorphism, *i.e.* on the retrograde path.

Parts of the rocks have suffered a strong retrogressive, but still syntectonic overprint with far-reaching re-equilibration and a transformation into muscovite-biotite gneisses with few relics of cordierite and sillimanite.

MINERAL CHEMISTRY

Mineral analysis was carried out for samples with metamorphic index mineral assemblages from all three zones in order to derive P-T- estimates; selected analyses are given in table 2. For analytical methods see appendix.

CORDIERITE

Cordierite is widespread in the high-grade metamorphic basement and was formed by reactions (3) in the eastern and western zones and by reactions (4), (5) or (6) in the central zone, in rare cases also in the western zone. Since Hensen & Green (1973) and Holdaway & Lee (1977), the X_{Mg} of cordierite has been used as a pressure indicator for cordierite

Tab. 2a – Selected microprobe analyses from indicative samples of all three zones. Cordierite (crd) was formed by reaction (3) in US-227 and MS-3475 of the eastern and western zone, respectively, by reaction (4) in HB-4 and by reaction (6) in HB-2, both samples from the central zone. Orthopyroxene (opx) of samples US-445 and HB-43 is partly replaced by cummingtonite (cum) and Ca-amphibole (Ca-am). Garnet (grt) stands in paragenesis with cordierite (HB-4) or with orthopyroxene (US-445). Garnet of sample HB-2 with diffusional Mg loss along the rims is going to be replaced by cordierite according to reaction (6). The spinels (spl) are typical for granulite-facies assemblages in the central zone. Cations were calculated on the oxygen number given in the table. Fe^{3+} for garnet, spinel and amphibole was calculated assuming an ideal site occupancy, for amphibole the midpoint of the possible range was taken.

	US-227	HB-4	HB-2	MS-3475	HB-4	US-445	HB-2	US-445	HB-43	US-445	HB-43	HB-43	WH2-44	WH4-3
wt.%	**crd**	**crd**	**crd**	**crd**	**grt**	**grt**	**grt**	**opx**	**opx**	**cum**	**cum**	**Ca-am**	**spl**	**spl**
SiO_2	48.15	49.24	48.51	48.14	38.06	38.10	37.43	49.81	51.60	52.65	54.06	50.26	<0.05	<0.05
TiO_2	<0.05	<0.05	<0.05	<0.05	<0.05	<0.05	<0.05	0.20	0.10	0.13	0.13	0.16	<0.05	<0.05
Al_2O_3	32.45	33.45	33.62	33.00	21.61	21.71	21.21	3.97	0.83	3.86	0.75	4.96	56.70	58.45
Cr_2O_3	-	-	-	-	<0.05	0.06	<0.05	<0.05	0.11	<0.05	<0.05	0.20	0.13	0.30
Fe_2O_3	-	-	-	-	0.15	<0.05	0.21	-	-	0.62	1.01	2.99	4.13	1.84
MgO	7.36	9.75	9.27	7.69	7.59	7.24	3.43	18.69	19.01	17.43	18.87	14.06	4.41	4.33
CaO	<0.05	<0.05	<0.05	<0.05	1.48	1.64	1.62	0.18	0.73	0.28	0.56	11.74	<0.05	<0.05
MnO	0.30	0.30	0.20	0.50	3.99	2.43	5.59	0.78	0.43	0.67	0.42	0.16	0.13	0.16
FeO	8.40	5.70	6.60	8.80	26.24	28.29	31.07	25.62	26.49	21.91	21.78	11.86	29.49	31.08
ZnO	-	-	-	-	-	-	-	-	-	-	-	-	4.89	3.61
Na_2O	0.90	0.15	0.09	0.20	-	-	-	<0.05	0.06	0.31	<0.05	0.38	-	-
K_2O	<0.05	<0.05	<0.05	<0.05	-	-	-	<0.05	<0.05	<0.05	<0.05	0.34	-	-
Total	**97.56**	**98.59**	**98.29**	**98.33**	**99.12**	**99.47**	**100.56**	**99.25**	**99.36**	**97.86**	**97.58**	**97.11**	**99.88**	**99.77**
Oxygens	**18**	**18**	**18**	**18**	**24**	**24**	**24**	**6**	**6**	**23**	**23**	**23**	**4**	**4**
Si	5.01	5.00	4.96	4.98	5.98	5.98	5.98	1.90	1.98	7.64	7.86	7.35	0.00	0.00
Al	3.99	4.00	4.05	4.02	4.00	4.02	4.00	0.18	0.03	0.66	0.13	0.85	1.91	1.95
Ti	0.00	0.00	0.00	0.00	0.00	0.00	0.00	0.01	0.00	0.01	0.01	0.02	0.00	0.00
Cr	-	-	-	-	0.00	0.01	0.00	0.00	0.00	0.00	0.00	0.02	0.00	0.01
Fe^{3+}	-	-	-	-	0.02	0.00	0.03	-	-	0.07	0.11	0.33	0.09	0.04
Mg	1.14	1.48	1.41	1.19	1.78	1.69	0.82	1.06	1.09	3.77	4.09	3.07	0.19	0.18
Ca	0.00	0.00	0.00	0.00	0.25	0.28	0.28	0.01	0.03	0.04	0.09	1.84	0.00	0.00
Mn	0.03	0.02	0.02	0.04	0.53	0.32	0.76	0.03	0.01	0.08	0.05	0.02	0.00	0.00
Fe^{2+}	0.73	0.48	0.56	0.76	3.45	3.71	4.15	0.82	0.85	2.66	2.65	1.45	0.70	0.74
Zn	-	-	-	-	-	-	-	-	-	-	-	-	0.10	0.08
Na	0.18	0.03	0.02	0.04	-	-	-	0.00	0.01	0.09	0.00	0.11	-	-
K	0.00	0.00	0.00	0.00	-	-	-	0.00	0.00	0.00	0.00	0.06	-	-
Total	**11.08**	**11.01**	**11.02**	**11.03**	**16.01**	**16.01**	**16.02**	**4.01**	**4.00**	**15.02**	**14.99**	**15.12**	**2.99**	**3.00**
X_{Mg}	0.61	0.75	0.72	0.61	0.34	0.31	0.16	0.57	0.56	0.58	0.60	0.63	0.19	0.19

Tab. 2b – Microprobe analyses from sample 26.1T17 of the western zone which were used for P-T calculations applying an internal consistent thermodynamic data set.

	Crd1	Crd1	Bt1	Bt2	Pl1	Pl1	Bt2	Crd2	Grt1	Grt1	Crd3	Bt4	Pl2	Pl2
wt.%	core	rim	incl.	foliation	core	rim	incl.	core	core	rim	near Grt	near Grt	core	rim
SiO_2	48.89	49.74	34.50	36.07	61.54	59.43	35.84	48.66	37.95	38.27	48.78	36.07	60.43	60.22
TiO_2	0.05	<0.05	3.62	3.21	<0.05	<0.05	3.25	<0.05	<0.05	<0.05	<0.05	3.36	<0.05	<0.05
Al_2O_3	34.15	34.00	20.43	20.77	25.99	26.27	20.54	34.17	22.46	22.09	33.92	20.32	25.62	26.38
Cr_2O_3	0.06	<0.05	<0.05	0.10	<0.05	<0.05	0.10	<0.05	<0.05	0.05	<0.05	0.26	0.05	<0.05
MgO	8.06	8.05	8.04	8.93	0.06	<0.05	8.87	7.80	4.80	3.35	8.29	9.34	<0.05	<0.05
CaO	<0.05	<0.05	0.11	<0.05	6.48	7.07	<0.05	<0.05	1.34	1.11	0.03	0.00	6.31	6.99
MnO	0.17	0.22	0.06	0.07	<0.05	<0.05	0.06	0.20	2.10	2.57	0.20	0.05	0.08	<0.05
FeO*	8.73	8.82	18.52	19.76	0.05	0.16	19.08	9.10	33.72	35.58	8.34	18.17	<0.05	<0.05
Na_2O	0.16	0.17	0.23	0.05	8.12	7.78	0.22	0.16	-	-	0.20	0.29	7.95	7.91
K_2O	<0.05	<0.05	8.61	9.27	0.26	0.16	9.32	<0.05	<0.05	<0.05	<0.05	9.20	0.30	0.20
Total	**100.27**	**101.00**	**94.12**	**98.23**	**102.50**	**100.87**	**97.28**	**100.09**	**102.37**	**103.02**	**99.76**	**97.06**	**100.74**	**101.70**
Oxygens	**18**	**18**	**22**	**22**	**8**	**8**	**22**	**18**	**24**	**24**	**18**	**22**	**8**	**8**
Si	4.95	4.99	5.27	5.30	2.67	2.63	5.31	4.94	5.88	5.96	4.95	5.34	2.67	2.64
Al	4.07	4.02	3.68	3.60	1.33	1.37	3.59	4.09	4.10	4.06	4.06	3.54	1.34	1.36
Ti	0.00	0.00	0.42	0.36	0.00	0.00	0.36	0.00	0.00	0.00	0.00	0.37	0.00	0.00
Cr	0.01	0.00	0.01	0.01	0.00	0.00	0.01	0.00	0.00	0.01	0.00	0.03	0.00	0.00
Fe^{3+}	0.00	0.00	0.00	0.00	0.00	0.00	0.00	0.00	0.18	0.03	0.00	0.00	0.00	0.00
Mg	1.22	1.20	1.83	1.96	0.00	0.00	1.96	1.18	1.11	0.78	1.25	2.06	0.00	0.00
Ca	0.00	0.00	0.02	0.00	0.30	0.34	0.00	0.00	0.22	0.19	0.00	0.00	0.30	0.33
Mn	0.02	0.02	0.01	0.01	0.00	0.00	0.01	0.02	0.28	0.34	0.02	0.01	0.00	0.00
Fe^{2+}	0.74	0.74	2.37	2.43	0.00	0.01	2.37	0.77	4.19	4.61	0.71	2.25	0.00	0.00
Na	0.03	0.03	0.07	0.01	0.68	0.67	0.06	0.03	-	-	0.04	0.08	0.68	0.67
K	0.00	0.01	1.68	1.74	0.01	0.01	1.76	0.00	0.01	0.00	0.00	1.74	0.02	0.01
Total	**11.03**	**11.02**	**15.34**	**15.41**	**5.01**	**5.02**	**15.44**	**11.03**	**15.96**	**15.98**	**11.04**	**15.41**	**5.01**	**5.02**
X_{Mg}	0.62	0.62	0.44	0.45	-	-	0.45	0.60	0.20	0.14	0.64	0.48	-	-

formation. Cordierite which formed according to reaction (3) in samples of the eastern and western zones shows comparable X_{Mg}-values, with sample averages varying between 0.58 und 0.65. Cordierite of sample 26.1T17 from the western zone (Eld Peak), which was used for P-T estimates with an internal consistent thermodynamic data set was also formed by reaction (3), the X_{Mg}-values vary between 0.60 and 0.62. Cordierite of the same sample formed by reaction (6) has an X_{Mg} of 0.64.

Cordierite of the central zone formed by reactions (4) and (5) and has significant higher sample averages between 0.67 und 0.75. The highest X_{Mg} of 0.75 was observed in sample HB-4 with euhedral cordierite and garnet in paragenesis. Comparable values were obtained for cordierite of the central zone resulting from reaction (6), scattering in sample averages between 0.67 and 0.76.

GARNET

In **orthopyroxene-free** mineral assemblages of the central zone, garnet is either more or less euhedral, or it is affected by corrosion which started from rims and cracks. Most of the analyzed garnet crystals contain inclusions of sillimanite and were formed by reaction (4). The corroded garnets are commonly replaced by cordierite along the rims in the course of reaction (6). All garnets are almandine-pyrope solid solutions with only minor contents of spessartine, andradite and grossulare end-members. They consist of large, chemically homogeneous core regions which make up by far the majority of the garnet volumes and which typically have pyrope contents between 26 and 33 mol% and almandine contents between 62 and 68 mol%. The spessartine content usually is 2 mol%, but in rare cases is 7-9 mol% at the expense of almandine. The euhedral garnets have very thin rims where retrograde diffusion has led to a slight increase of almandine (64-71 mol%) at the expense of pyrope (22-30 mol%). A few garnets, *e.g.* those of HB-4 which are in equilibrium with euhedral cordierite, have almost no zonation. Corroded garnets have similar core compositions, the rims of these garnet relics (which are not the original rims of the garnet grains), however, show a pronounced pyrope loss (14-24 mol%) and almandine gain (70-80 mol%).

A further group of euhedral garnets without sillimanite-inclusions, but with oriented biotite-inclusions, is depleted in pyrope, if compared with garnet described above. Core compositions are 14-21 mol% pyrope, 54-76 mol% almandine and 4-12 mol% spessartine, rim compositions show even less pyrope (10-16 mol%), but more almandine (68-79 mol%) and spessartine (5-20 mol%).

Garnet of sample 27.1T17 from Eld Peak in the western zone is composed of 73 mol% almandine, 19 mol% pyrope, 5 mol% spessartine and 4 mol% grossular in the core, varying to 78 mol% almandine and 13 mol% pyrope at the rim.

Orthopyroxene-bearing assemblages are commonly free of garnet. In few samples, however, garnet is either in direct contact with orthopyroxene or was in contact with orthopyroxene, but is now separated by an alteration rim, or it belongs to the paragenesis, but without direct contact with orthopyroxene. In all situations, the compositions of garnets are similar: in their cores, the garnets contain pyrope between 25 and 36 mol%, almandine between 57 and 69 mol% and spessartine between 2 and 7 mol%. At their rims and also in very small relics, these garnets are composed of 16-28 mol% pyrope, 59-73 mol% almandine and 3-8 mol% spessartine. With these chemistries, the garnets in orthopyroxene-bearing assemblages do not significantly differ from those of the orthopyroxene-free assemblages.

PYROXENE

The range in orthopyroxene compositions of 13 samples is 51-58 mol% enstatite, 41-48 mol% ferrosilite and 0-2 mol% others, mainly the Mn-end member. There is no difference between orthopyroxene in garnet-bearing assemblages and orthopyroxene in garnet-free ones. Clinopyroxene coexisting with orthopyroxene in one sample is diopside with 38 mol% enstatite, 16 mol% ferrosilite and 46 mol% wollastonite endmembers. Orthopyroxene is often replaced by amphibole along broad rims and sometimes is completely pseudomorphed by these phases. This amphibole is anthophyllite or cummingtonite in a first generation and magnesiohornblende to actinolite in a second generation.

THERMOBAROMETRY

The lack of index mineral assemblages makes it difficult for many samples to estimate metamorphic conditions. A few samples from all three zones that contain assemblages with *e.g.* cordierite, sillimanite, biotite, garnet can be used for thermobarometry.

CORDIERITE AND CORDIERITE + GARNET THERMOBAROMETRY

Hensen & Green (1973) and Holdaway & Lee (1977) quantified the pressure-dependent Fe-Mg substitution in cordierite as a tool for P-estimates in metamorphic rocks. In the working area, cordierite was formed by reactions (3), (4) and (6) and therefore may allow for a comparison of metamorphic pressures between the different zones or the different stages of metamorphic evolution, respectively.

In the eastern and western zones, cordierite was almost exclusively formed by reaction (3). From its X_{Mg}-values a pressure range between 2.5 and 5.5 kbar at temperatures between about 600 and 835°C may be

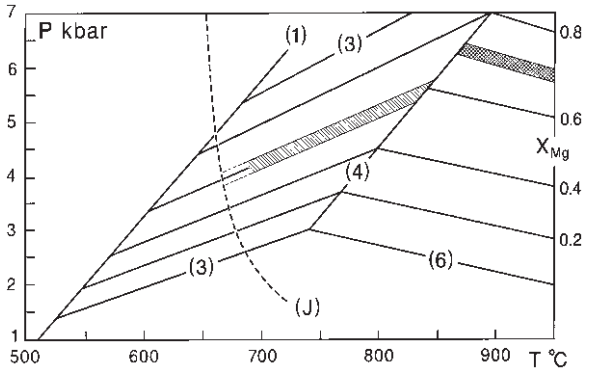

Fig. 2 – Cordierite-forming mineral reactions and X_{Mg}-isopleths of cordierite in the P-T field at $P_{H2O}=P_{tot}$ (Holdaway & Lee, 1977). The hatched field displays the composition of cordierite in the eastern and western zones, the squared field the composition of cordierite in the central zone. For numbers of reactions see text. (J), solidus of the quartz – orthoclase – plagioclase (An_{40}) – H_2O system (Johannes, 1984).

deduced ($P_{H2O}=P_{tot}$). However, the cordierite-bearing rocks are associated with metatexites. Therefore the pressure/temperature range is limited to lower values by the solidus of the quartz – orthoclase - plagioclase (an_{40}) - H_2O system (Johannes 1984) and reduced to a range of 4-5.5 kbar/700-835°C. A limit to higher temperatures is given by reaction (4) which did not take place except for samples 27.1T8 and 28.1T13 (Fig. 2).

Cordierite of the central zone which clearly results from reaction (6) shows X_{Mg}-values between 0.67 and 0.76 (except RK-9 with 0.62). This cordierite grew at around 6 kbar and a minimum temperature of 860°C, as deduced from the grid of Holdaway & Lee for $P_{H2O}=P_{tot}$ (1977; Fig. 2). According to Martignole & Sisi (1981) and Harley et al. (2002), the pressure estimate is strongly dependent from the volatile content (H_2O + CO_2) of the cordierite. Using the calibration of Martignole & Sisi (1981), isopleths for coexisting cordierite and garnet in the investigated samples intersect at about 800°C independent from H_2O, however, at 5 kbar for H_2O-free cordierite and at 8-9 kbar for cordierite with nH_2O of 0.8. The 0.8 molecules H_2O p.f.u. saturation isopleth of Harley et al. (2002) conforms to a pressure of 8 kbar at 800°C. Microprobe analyses with generally low totals for the cordierite investigated point to enhanced volatile contents in the crystal lattice, correlating to a medium pressure level above 5-6 kbar. However, taking into account the cordierite data presented, Harley (pers. comm.) expects pressure conditions for these cordierites below 8-9 kbar.

In the western zone, cordierite of sample 26.1T17 formed by reaction (6) shows an X_{Mg} of 0.64 which closely resembles the composition of those cordierites from the central zone and points to similar granulite-facies P-T conditions.

A temperature estimate was carried out for the assemblage cordierite + garnet at three locations in sample HB-4 from the central zone (Harald Bay). The assemblage is in textural equilibrium, the mineral grains show only slight chemical zonation, and the sample is interpreted to represent more or less the highest temperature stage of metamorphism. The geothermometer of Bhattacharya et al. (1988) was used, calibrated for the temperature-dependent exchange of Fe and Mg between cordierite and coexisting garnet. Assuming a pressure of 8 kbar, calculated temperatures range between 810 and 850°C, when the garnet core compositions were used. Taking the rim compositions, the values are 760-780°C (Tab. 3).

ORTHOPYROXENE + GARNET THERMOBAROMETRY

A number of samples exclusively from the central zone contain orthopyroxene in an assemblage with biotite + plagioclase + quartz. Following Bucher & Frey (1994), the orthopyroxene-in isograd in the KFASH-system above a pressure of 4 kbar is almost pressure-independent and located at 780°C, H_2O- and quartz-saturation assumed. Spear (1993) describes orthopyroxene-bearing assemblages in metapelites to occur above a temperature of 800°C. These values give a minimum temperature for the investigated assemblages.

Four samples of the central zone contain unaltered or nearly unaltered assemblages of orthopyroxene +

Tab. 3 – Results of conventional thermobarometry: Temperatures calculated for the texturally equilibrated assemblage garnet + cordierite, observed at 3 locations of sample HB-4, assuming pressures of 5 and 8 kbar. Average pressure and temperature values and variation of the individual calculations for orthopyroxene-garnet assemblages found in four samples of the central zone. Temperatures calculated for retrograde muscovite-biotite assemblages of four samples, assuming 2 and 3 kbar pressure.

Sample	Garnet-cordierite-thermometer				
	T core [°C]		T rim [°C]		
	5 kbar	8 kbar	5 kbar	8 kbar	
HB-4 / 1	791	807	763	779	
HB-4 / 2	809	825	746	761	
HB-4 / 3	833	850	763	779	
	Orthopyroxene-garnet thermobarometer				
	Average ± 1σ		Variation		n
	P [kbar]	T [°C]	P	T	
US-445	9.5 ± 0.6	773 ± 14	8.5-10.3	752-792	6
WH2-11	9.7 ± 0.9	801 ± 20	8.1-11.4	770-836	16
WH2-20	8.4 ± 0.9	869 ± 23	7.2-10.5	834-934	48
WH3-3	8.0 ± 0.7	840 ± 22	7.0- 9.0	811-874	9
	Muscovite-biotite thermometer				
	T [°C] Average ± 1σ		T [°C] Variation		n
	3 kbar	2 kbar	3 kbar	2 kbar	
US-351	515 ±16	496 ±17	499-544	480-527	10
WH2-32	514 ±19	495 ±20	490-545	469-527	13
WH2-36	520 ± 7	500 ± 7	507-532	488-513	20
MS-3495	491 ± 4	471 ± 4	486-495	466-476	4

garnet (US-445, WH2-11, WH2-20, WH3-3). For these, pressure estimates were carried out using the geobarometer of Carswell & Harley (1990) which is based on a pressure-dependent exchange of Al in orthopyroxene, coexisting with garnet. Temperature estimates were done by a geothermometer of Lee & Ganguly (1988), using the temperature-dependent Mg-Fe exchange between coexisting orthopyroxene and garnet. The averages of pressure values, calculated for several locations of each of the four samples, range between 8.0 and 9.7 kbar, the temperatures between 770 and 870°C (Tab. 3).

THERMOBAROMETRY USING A THERMODYNAMIC DATA SET

In sample US-495 from the central zone (Mt. Archer), the paragenetic mineral assemblage biotite + cordierite + sillimanite + spinel + plagioclase + quartz was analyzed in detail. P-T conditions for the formation of this assemblage were calculated using the THERMOCALC method of Powell & Holland (1994), based on a new version of the internally consistent thermodynamic set of data from Holland & Powell (1990). Pressures of seven calculations vary between 7.5 and 8 kbar, for temperatures between 787 and 837°C and at $X_{H2O} = 1$. The pressure values are lowered by 1 kbar and 50°C for $X_{H2O} = 0.6$. (For more details of these investigations see Schüssler et al., 1999).

New P-T data were obtained using THERMOCALC for the mineral assemblage garnet + cordierite + sillimanite + biotite + plagioclase + K-feldspar + quartz for the sample 26.1T17 which was taken from Eld Peak in the Lazarev Mountains of the western zone. The P-T calculation was carried out using the core compositions of the minerals in the first instance and the rim compositions in a second case, and taking into account various values for an X_{H2O} between 1.00 and 0.25. The microprobe analyses used for the calculations are given in table 2b and full results are shown in table 4. Taking the "core"-data, all calculated temperatures are above 800°C and therefore show clear granulite-facies conditions at medium pressures of 5 to 8 kbar. Using the "rim"-data, granulite-facies temperatures are still reached, at low to medium pressures.

MUSCOVITE AND MUSCOVITE + BIOTITE THERMOBAROMETRY

In all three zones there are samples which are strongly affected by a retrograde overprint. This led to formation of secondary, late muscovite, in part together with biotite. The presence of the critical paragenetic assemblage biotite + muscovite + K-feldspar + quartz in most of the samples allows for application of the phengite barometer of Massonne & Schreyer (1987). From very low Si-contents of the muscovite between 6.02 and 6.12 p.f.u. and the upper thermal stability of muscovite, given by several muscovite-consuming reactions, maximum P-T conditions for the formation of the retrograde muscovite are 3 kbar/650°C.

Four samples, two from the central zone, one from the eastern and one from the western zone, contain abundant retrograde muscovite + biotite in textural equilibrium. These samples represent higher grade gneisses which were almost completely reworked to form retrograde muscovite - biotite schists. Muscovite - biotite pairs from textural domains in every sample were analyzed and, using the geothermometer of Hoisch (1989), the temperature conditions for the formation of these muscovite - biotite assemblages were calculated (Tab. 3). They range between 490 and 520°C, assuming the maximum possible pressure of 3 kbar (for 2 kbar, the temperatures are between 470 and 500°C; it should be noted, that the pre-requisites given by Hoisch, 1989, for the application of the thermometer are fullfilled for the samples investigated).

RADIOMETRIC AGE DETERMINATIONS

Schüssler et al. (1999) carried out U-Pb age determinations on monazites and biotites from partly retrograded very-high-grade metamorphic rocks from the central zone of the Oates Coast basement complex. Monazites from samples US-380 (Thompson Peak), US-495 (Mt. Archer) and US-501 (Harald Bay) yielded concordant and close to concordant ages between 484 and 494 Ma, which were interpreted as minimum ages for the last high-temperature metamorphism in this geological unit. Biotites from the same samples yielded Rb-Sr, K-Ar and Ar-Ar ages in the range of 476 - 470 Ma. The geological significance of the biotite ages is corroborated by Ar-Ar plateau ages of 472±2 Ma of two muscovite concentrates from a syn- to late-tectonic pegmatite of Ringgold Knoll in the central zone (Schüssler & Henjes-Kunst, 1994, Schüssler et al., 1999).

New age determinations were performed to provide additional geochronological constrains for the tectonometamorphic evolution of the basement complex and adjacent areas in the northwestern Wilson Terrane. Amphiboles from amphibolites of all three zones, muscovite and biotite from the Archangel granite and muscovite from two late-tectonic pegmatites, which cross-cut the Wilson and the Lazarev Thrust systems of the eastern and the western zone, respectively, were dated by the ^{40}Ar-^{39}Ar incremental-heating method. For analytical methods see appendix.

AMPHIBOLES

From the eastern zone, two grain-size fractions of amphibole (125-63 µm and 250-125 µm) of the

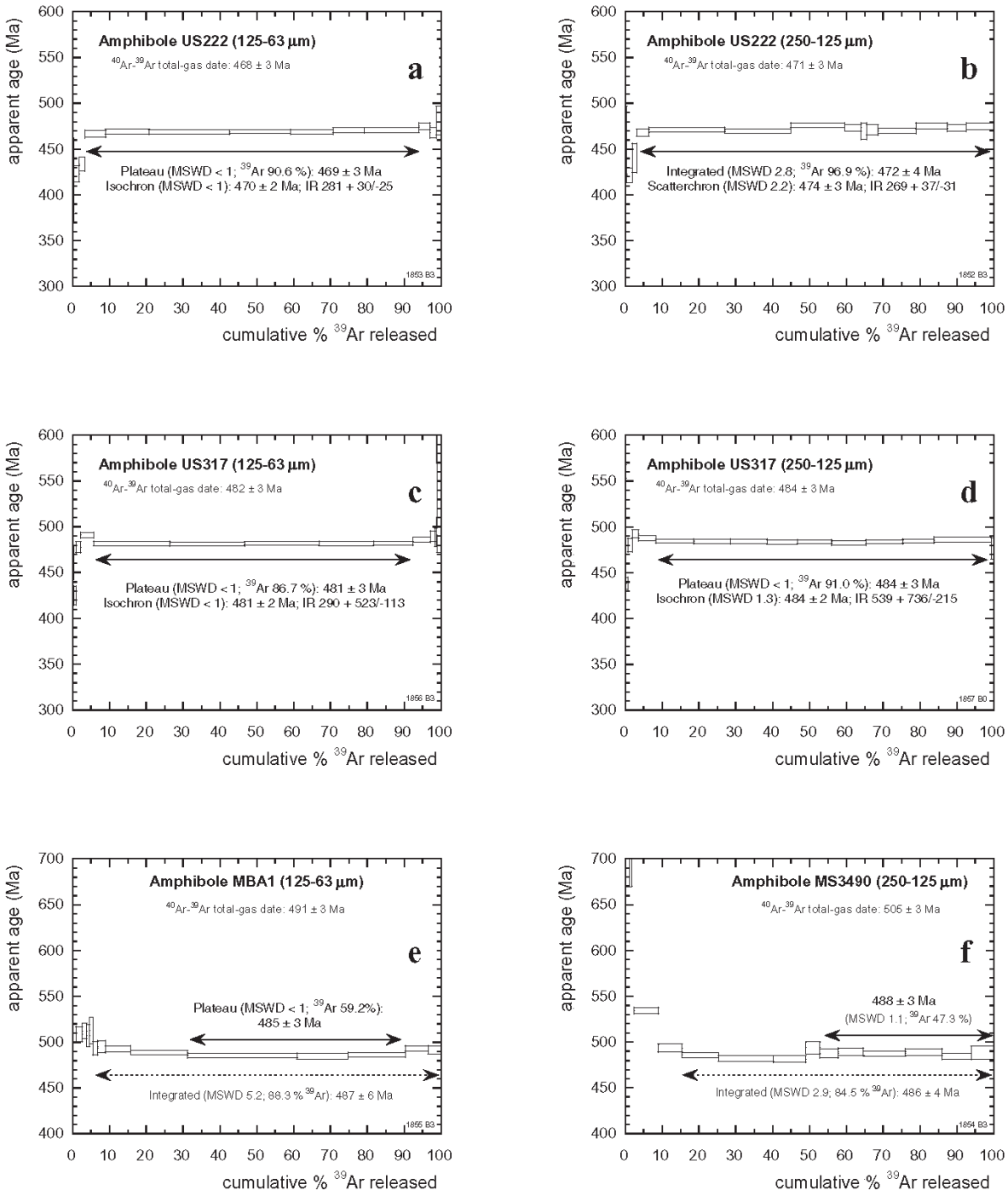

Fig. 3 – ^{40}Ar-^{39}Ar age spectra of amphibole fractions: (a, b) amphibolite sample US-222, height-point 1250 westsouthwest of Mt. Shields, eastern zone, (c, d) amphibolite sample US-317, eastern Exiles Nunatak, (e) ultramafic sample MBA-1, Mt. Blowaway area, central zone, (f) amphibole gabbro sample MS-3490, Burnside Ridge, western zone.

amphibole gneiss US-222 from height-point 1250 west-southwest of Mt. Shields were dated. The 125–63 µm fraction yields for about 91 % of the released gas identical Ar-Ar plateau and isochron ages of 469±3 Ma and 470±2 Ma, respectively (Fig. 3a). The 250–125 µm fraction gave a slightly more disturbed age spectrum (Fig. 3b). Integration of the flat part of the spectrum including about 97 % of the released gas yields an age of 472±4 Ma corresponding to an errorchron age of 474±3 Ma.

From the central zone, amphiboles from two samples were dated. Two different amphibole size fractions from sample US-317, an amphibolite layer from the eastern Exiles Nunatak, yield well-defined Ar-Ar age plateaus and isochrons for about 87 – 91 % of the released gas. The plateau and isochron ages vary between 484±3 and 481±3 Ma (Figs. 3c and d). The amphibole concentrate of sample MBA-1, a gabbroic olivine-amphibole rock from height-point 1170 southwest of Mt. Blowaway, gave a somewhat

stronger disturbed Ar-Ar spectrum probably due to the presence of some excess argon. Only three heating steps covering about 59 % of the released ^{39}Ar define a plateau age of 485±3 Ma (Fig. 3e). From the western zone, only one amphibole concentrate of sample MS-3490, a coarse-grained amphibole gabbro from the southern part of Burnside Ridge, was dated. It yields a moderately disturbed Ar-Ar spectrum with strongly elevated ages for the first low-temperature steps indicative of excess argon (Fig. 3f). The second half of the spectrum defines a plateau over 6 heating steps and almost 50 % of the ^{39}Ar released, giving an age of 488±3 Ma. Including further 4 steps covering in total 85 % of the released ^{39}Ar, an integrated age of 486±4 Ma can be calculated.

MICAS

The Archangel Nunataks are predominantly made up by the post-tectonic Archangel granite which intruded the low-grade metasedimentary Berg Group occurring to the west of the western zone (Fig. 1a, b). Muscovite from sample US-401a, from a small nunatak immediately west of the largest Archangel Nunatak (*i.e.* Outrider Nunatak), was Ar-Ar dated in two grain-size fractions. These define ideal plateaus and isochrons covering about 92 % of the released ^{39}Ar and resulting in identical ages of on average 482±2 Ma (Figs. 4a and b). Two biotite fractions from the same sample gave strongly disturbed ages (Figs. 4c and d). Their medium-temperature steps, however, define plateaus over 52 and 72 % of the released ^{39}Ar with ages of 484±3 and 483±3 Ma, respectively.

The pegmatite 930216-3 from Stevenson Bluff located in the eastern zone intruded the thrust plain of the Wilson Thrust, pegmatite 930211-7 from North Nunatak located in the western zone intruded the Lazarev Thrust. Muscovites of both pegmatites displays almost ideal Ar-Ar spectra defining plateaus over 16 heating steps and 99.7% of ^{39}Ar released (Fig. 4e, f), with ages of 466±2 Ma for the Stevenson Bluff and of 472±2 Ma for the North Nunatak pegmatite.

REGIONAL AGE DISTRIBUTION

A compilation of the new data together with those of Schüssler et al. (1999) is given in table 5. Although the geochronological data base for the three zones of the Oates Coast basement complex is still limited, a general trend is evident, with mineral ages becoming younger from west to east. This holds true for the amphibole as well as for the mica data. It is notable that the amphibole ages are several million years older than corresponding mica ages from the respective zone. Amphiboles from the western zone record ages of 488 – 486 Ma, those from the central zone 485 – 481 Ma and those from the eastern zone 472 – 469 Ma. The mica ages are 484 – 482 Ma for the Archangel Granite west of the western zone, 472 for the late-tectonic pegmatite in the western zone, 476 – 470 Ma for metamorphic rocks and a syn- to late-tectonic pegmatite from the central zone and 466 Ma for the late-tectonic pegmatite in the eastern zone.

PRESSURE-TEMPERATURE-TIME EVOLUTION

The new results of thermobarometric calculations and geochronological investigations give more insight into the P-T-t evolution of the Oates Coast basement complex as a whole. Clear differences in the metamorphic evolution of the various zones become obvious, when the data are integrated.

EASTERN AND WESTERN ZONES

Petrological results indicate that the eastern zone and parts of the western zones have experienced a very similar metamorphic evolution. The lowest-grade rocks of these two zones contain primary muscovite associated with quartz, as well as biotite associated with sillimanite, indicating that reactions (1) and (3) have not taken place. Using the position of reaction (1) in the P-T field (Xu et al., 1994), these rocks did not experience temperatures in excess of 700°C, if a pressure of 4 to 5.5 kbar and $X_{H2O}=1$ is assumed. For most of the pelitic rocks, however, reaction (3) proceeded to completion. The metamorphic P-T conditions for the formation of critical mineral assemblages occurring in these rocks are 4-5.5 kbar/700-840°C, if $X_{H2O}=1$. For $X_{H2O}<1$, the temperature range would be reduced from both sides to a value of about 750°C, parallel to a pressure decrease. Evidence for still higher-grade metamorphic conditions in parts of the western zone, *i.e.* the area between Eld Peak and Rescue Nunatak, are relics of sillimanite in garnet which indicate that reaction (4) has taken place. P-T calculations on one sample from Eld Peak clearly point to temperatures above 800°C at medium pressures of around 7 to 8 kbar. The replacement of garnet by cordierite according to reaction (6), as observed in several samples of the western zone, is the consequence of a more or less isothermal pressure decrease at granulite-facies temperatures.

The high-grade metamorphic event has not yet been dated for these zones. P-T conditions of 2-3kbar/~500°C could be estimated for the retrograde formation of secondary muscovite and of muscovite+biotite assemblages in some of the metamorphic rocks.

The metamorphic basement of the eastern and western zones has been formed during a high-temperature/low-pressure metamorphism that reached upper amphibolite facies to lower granulite facies. In

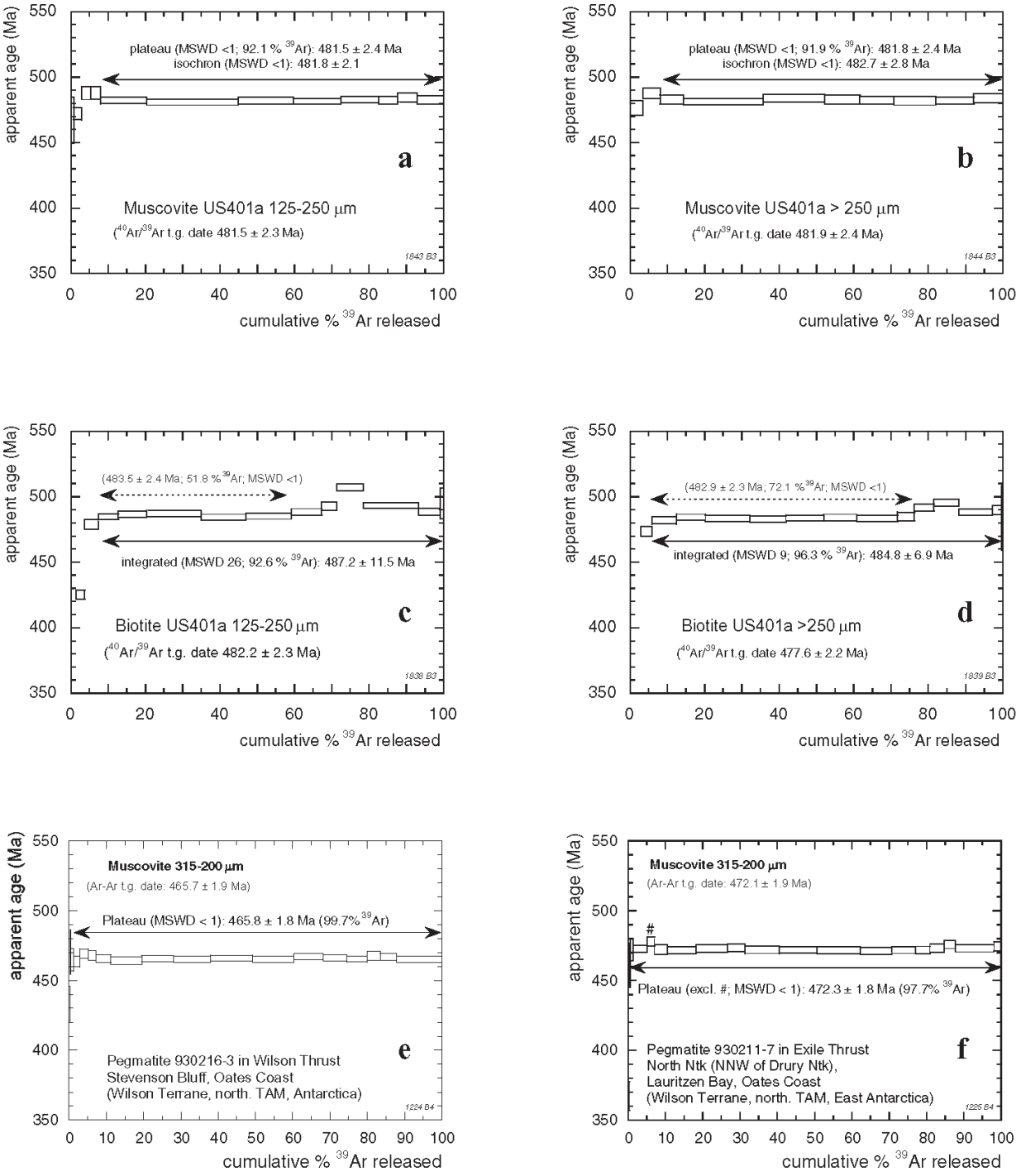

Fig. 4 – ^{40}Ar-^{39}Ar age spectra of muscovite (a, b) and biotite (c, d) fractions from granite sample US-401a, Outrider Nunatak area, Archangel Nunataks, of muscovite (e) from a pegmatite at Stevenson Bluff, eastern zone, of muscovite (f) of a pegmatite from North Nunatak, western zone.

addition, some of the typical low- to medium-pressure granulite-facies mineral assemblages as have been found in the central zone occur in parts of the western zone. A clockwise P-T path is suggested by the formation of cordierite through reaction (3), and in the western zone also through reaction (6). In cases, rocks of lower metamorphic grade occur, but without a regional correlation within the zones. A retrograde overprint with formation of muscovite +biotite took place at about 500°C. According to Villa (1998), the closure temperature for the K-Ar system in micas is about 450 - 500°C**.** Therefore, the Ar-Ar mica age of 466±2 Ma in the eastern zone may closely date the time of retrograde overprint in the eastern zone. It should be noted, however, that these dated micas of the eastern zone derive not directly from retrograde metamorphic rocks, but from a small late-tectonic pegmatite. For the western zone, the

Tab. 4a - Average pressure-temperature calculations on the interpreted peak assemblage for sample 26.1.00T17 (garnet-plagioclase-sillimanite-biotite-cordierite-microcline-quartz, using core compositions).

(i) The activity data for mineral end-members in the rock.

	py	**gr**	**alm**	**an**	**phl**	**ann**	**east**
a	0.00950	9.90e-5	0.330	0.430	0.0246	0.0380	0.0380
σ (ln a)	0.55915	0.81866	0.15091	0.15000	0.42655	0.39657	0.38888
	crd	**fcrd**	**sill**	**mic**	**q**	**H_2O**	
a	0.440	0.140	1.00	1.00	1.00	1.00	
σ (ln a)	0.15000	0.23500	0	0	0		

(ii) An independent set of reactions involving the mineral end-members.

1) gr + 2sill + q = 3an
2) 2py + 4sill + 5q = 3crd
3) 2alm + 4sill + 5q = 3fcrd
4) py + 5phl + 12sill = 5east + 4crd
5) east + 2crd = 2py + 3sill + mic + H_2O
6) 5ann + 6fcrd = 9alm + 3sill + 5mic + 5H_2O

(iii) Calculations for the independent set of reactions, for the given activity data and a (H_2O) = 1.0

	P(T)	**σ(P)**	**a**	**σ(a)**	**b**	**c**	**ln K**	**σ(ln K)**
1)	5.8	1.44	27.60	0.60	-0.11527	5.253	6.688	0.934
2)	5.6	0.99	-45.70	1.07	-0.06716	9.935	6.850	1.205
3)	5.0	0.59	90.38	1.09	-0.11622	10.730	-3.681	0.767
4)	3.9	2.23	-19.68	16.84	-0.05940	13.228	3.547	3.000
5)	7.6	1.48	104.61	3.45	-0.01551	-7.049	-4.401	1.221
6)	7.4	0.93	-35.89	5.69	0.07731	-25.061	18.170	2.786

(iv) Average PT calculated from the intercepts of the reactions, showing the effect of varying a (H_2O). For 95% confidence, fit (=χ2) should be < 1.54:

x(H_2O)	**P(kbar)**	**σ**	**T (°C)**	**σ**	**cor**	**χ2**
1.00	7.7	1.9	1015	142	0.893	1.52
0.75	7.0	1.5	969	116	0.886	1.36
0.50	6.2	1.2	916	92	0.882	1.17
0.25	5.1	0.9	822	66	0.879	0.90

mica age of 472±2 Ma of a pegmatite does not differ from mica ages of the central zone, but is clearly some 6 Ma older than that of the eastern zone. The Ar-Ar amphibole ages of 488-486 Ma for the western zone and 472-469 Ma for the eastern zone date some intermediate stage between peak metamorphism and retrograde formation of secondary mica. The differences in Ar-Ar amphibole ages imply that cooling in the eastern zone was delayed by some 16 million years compared to the western zone, given similar amphibole compositions.

CENTRAL ZONE

The rocks of the central zone contain much more evidence for a medium-pressure granulite-facies event than reported previously by Schüssler (1996) and Schüssler et al. (1999). The assemblage orthopyroxene + K-feldspar + plagioclase + quartz provides a lower temperature limit at about 800°C (orthopyroxene-in isograde of Bucher & Frey, 1994). Orthopyroxene – garnet thermobarometry resulted in P-T conditions of 8-9.7 kbar/770-870°C. For orthopyroxene-free rocks, the assemblage garnet + cordierite as a result of reaction (4) occurs over a wide field of the granulite facies (Spear, 1993). Reaction (4) requires minimum temperatures of 700°C if the pressure is >4 kbar and 800°C at P>8 kbar (KFMASH, Xu et al., 1994). Garnet-cordierite thermometry using equilibrium assemblages of sample HB-4 resulted in a temperature range of 810-850°C at 8 kbar and 790-850°C for pressures above 5 kbar (Tab. 3), if core compositions are used for calculations. These pressures and temperatures are corroborated by thermodynamic calculations on the assemblage biotite + cordierite + sillimanite + spinel + plagioclase + quartz using the method of Powell & Holland (1994), which gave P-T conditions of 7.5-8 kbar/790-840°C (Schüssler et al., 1999) (all P-T-t data compiled in Fig. 5).

In a few samples, the replacement of garnet + sillimanite by cordierite has been observed. This is inferred to reflect reaction (6) which is a decompressive reaction. From cordierite compositions, P-T conditions of ~6 kbar/>860°C can be estimated, assuming P_{H2O}=1 (5 kbar/>720°C for P_{H2O}=0.4). Taking cordierite-garnet assemblages of reaction (6), 8-9 kbar/~800°C results for a H_2O-rich system (5-6 kbar /~800°C for a H_2O-poor system). These

Tab. 4b - Average pressure-temperature calculations on the interpreted peak assemblage for sample 26.1.00T17 (garnet-plagioclase-sillimanite-biotite-microcline-cordierite-quartz, using rim compositions).

(ii) The activity data for mineral end-members in the rock.

	py	**gr**	**alm**	**crd**	**fcrd**	**phl**	**ann**
a	0.00320	4.70e-5	0.450	0.420	0.150	0.0340	0.0350
σ (ln a)	0.65429	0.83621	0.15000	0.15000	0.22524	0.39913	0.40751
	east	**an**	**sill**	**mic**	**q**	**H_2O**	
a	0.0440	0.470	1.00	1.00	1.00	1.00	
σ (ln a)	0.37671	0.10000	0	0	0		

(ii) An independent set of reactions involving the mineral end-members.

1) gr + 2sill + q = 3an
2) 2py + 4sill + 5q = 3crd
3) 2alm + 4sill + 5q = 3fcrd
4) py + 5phl + 12sill = 4crd + 5east
5) 2crd + east = 2py + 3sill + mic + H_2O
6) 6fcrd + 5ann = 9alm + 3sill + 5mic + $5H_2O$

(iii) Calculations for the independent set of reactions, for the given activity data and a (H_2O) = 1.0

	P(T)	**σ (P)**	**a**	**σ (a)**	**b**	**c**	**ln K**	**σ (ln K)**
1)	3.3	1.23	28.39	0.59	-0.11608	5.267	7.700	0.888
2	4.1	1.00	-43.39	1.05	-0.07116	10.118	8.887	1.384
3)	4.0	0.50	92.68	1.08	-0.12073	10.908	-4.094	0.739
4)	3.6	1.58	35.74	2.35	-0.12279	13.327	3.564	2.884
5)	6.1	1.41	94.14	0.86	-0.00234	-7.188	-6.631	1.394
6)	7.5	0.82	11.73	5.46	0.03204	-25.626	20.958	2.793

(iv) Average PT calculated from the intercepts of the reactions, showing the effect of varying a (H_2O). For 95% confidence, fit (=χ2) should be < 1.54:

x(H2O)	**P (kbar)**	**σ**	**T (°C)**	**σ**	**cor**	**χ2**
1.00	6.8	2.2	946	164	0.898	1.93
0.75	6.1	1.8	901	136	0.894	1.73
0.50	5.4	1.4	848	107	0.896	1.49
0.25	4.3	1.0	758	64	0.899	1.05

pressures estimated for the retrograde reaction (6) underscore the higher pressure values for the pressure peak of metamorphism.

The metamorphic rocks of the central zone were formed under medium-pressure granulite-facies conditions at about 8 kbar/>800°C. Hence they fit into the P-T field of 7.5±1 kbar and 800±50°C, which is typical for most of the known granulites (Bohlen, 1987) and which includes almost 50 % of P-T data of granulite-facies rocks (Harley, 1989). This metamorphic stage was followed by an almost isothermal decompression within a clockwise oriented P-T path, as shown by the P-T conditions of >5kbar/>800°C deduced for reaction (6). Retrograde Fe-Mg zoning of garnet and the late growth of euhedral Mg-poor garnet in some samples as well as the replacement of orthopyroxene by amphiboles may have occurred during this decompression stage. Ar-Ar amphibole ages of 485-481 Ma of the central zone most likely date the end of this phase of the P-T path, as the rocks cooled through 650-550°C (Villa, 1998).

Tab. 5 – Regional distribution of ages obtained by ^{40}Ar-^{39}Ar incremental heating experiments on amphiboles and micas.

	Archangel Granite	Western Zone	Central Zone	Eastern Zone
Amphibole		488 ±3 (486 ±4)	485 ±3 484 ±3 481 ±3	472 ±4 469 ±3
Muscovite	482 ±2 482 ±2	472 ±2	472 ±2	466 ±2
Biotite	483 ±2 484 ±2		476 ±2 472 ±3 470 ±2	

In the course of the isothermal decompression, the peak of anatexis should have been reached. Most probably, however, partial melting has started earlier, *i.e.* during the medium-pressure granulite-facies stage, even if the H_2O-activity was low. The solidus of the quartz-albite-orthoclase-H_2O-CO_2 system under granulite-facies conditions is reached at H_2O activities between 0.3 and 0.5 (Johannes & Holtz, 1990, 1996). Maximum activities of 0.4-0.5 can be assumed to initiate partial melting of the central zone granulites. The deduced P-T conditions for these granulites are

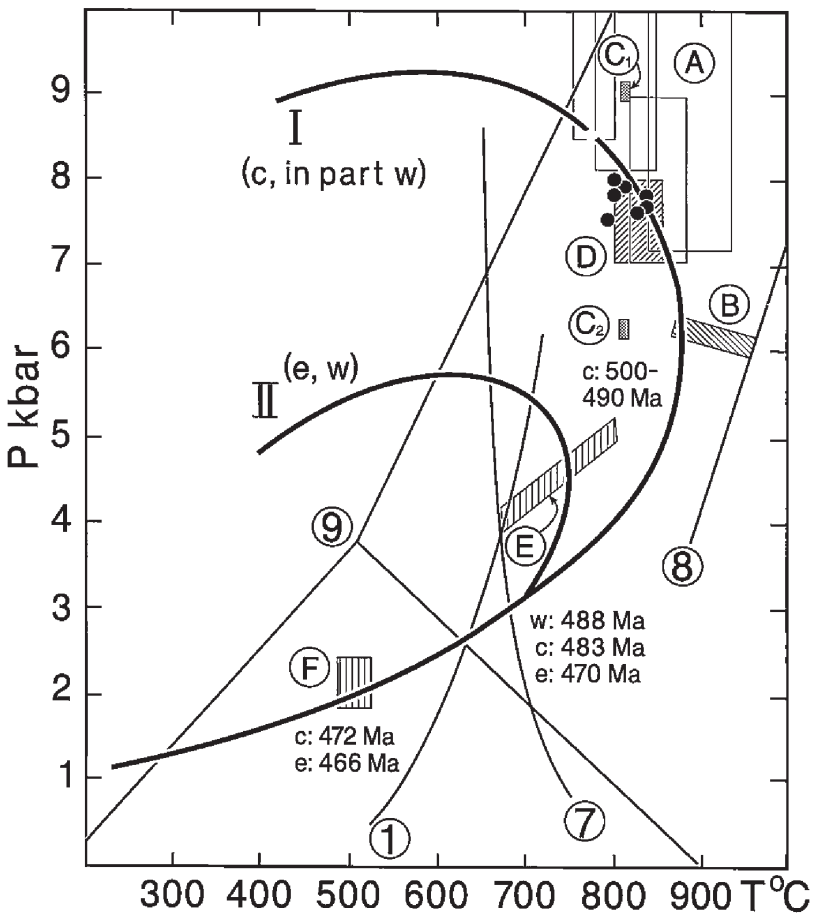

Fig. 5 – P-T-t evolution of metamorphic rocks in the Oates Coast basement complex. Path I is derived from granulite-facies rocks of the central zone and from the newly detected granulite-facies rocks in parts of the western zone. Path II is representative for most of the rocks in the eastern and western zones. Age data are distinguished for the eastern (e), central (c) and western (w) zone.
(1) muscovite + quartz = sillimanite + K-feldspar + vapour (Chatterjee & Johannes, 1974; Xu et al., 1994); **(7)** solidus of the quartz – K-feldspar – anorthite$_{40}$ – H_2O – system (Johannes, 1984); **(8)** garnet + cordierite + sillimanite = spinel + quartz (Spear, 1993; upper stability of the observed assemblages); **(9)** aluminum-silicate triple point (Holdaway & Mukhopadhyay, 1993); **(A)** variation of garnet – orthopyroxene thermobarometric calculations derived from four samples; **(B)** position of cordierites formed in the central zone (see also Fig. 2; Holdaway & Lee, 1977); **(C)** intersection of X_{Mg}-isopleths of garnet = 0.3 and cordierite = 0.7, assuming nH_2O = 0.8 (C_1) and 0.5 (C_2) (after Martignole & Sisi, 1983); **(D)** variation of garnet – cordierite thermometric calculations derived from sample HB-4; **(E)** position of cordierites formed in the eastern and western zones (see also Fig. 2; Holdaway & Lee, 1977); **(F)** variation of biotite – muscovite thermobarometric calculations derived from four samples of all three zones; black dots show results of thermobarometric calculations on sample US-495 of the central zone using an internal consistent thermodynamic data set (Schüssler et al., 1999).

located clearly above the dry-melting curve for pelites of Thompson & England (1984). Realistic H_2O activities are not definitely known for the moment, however, the metamorphic reactions mainly producing the granulite-facies assemblages are dehydration reactions, releasing H_2O to initiate partial melting. In addition, melt could have been produced directly instead of vapour during the metamorphic reactions (S. Harley, pers. comm.).

Isothermal decompression starting from a medium-pressure granulite-facies stage is a typical result of crustal thickening caused by continent-continent collision (*e.g.* Harley, 1989). Further results of such a collision are reinforced partial melting and complex magmatic processes (Wilson, 1989), with a peak of granite formation during the latest stage of collision (Hall, 1987). This is caused by intensive release of water during regional metamorphic overprint and dehydration of the primarily cold upper part of the lower, underthrusting continental plate, initiating extensive partial melting at the hot bottom of the overlying upper continental plate (Le Fort, 1981). According to a geotectonic model of Matzer (1995) for the Ross Orogeny, the Wilson Terrane was underthrusted by continental crust which may have been the base of the Bowers und Robertson Bay terranes. Possibly the fluids derived from this material caused intensive partial melting especially in the central zone which, together with parts of the western zone, at that time was the deepest level of the presently exposed overlying crust. The migmatites, diatexites and in-situ granitoids described above were formed during this stage. Diverging from Matzers´s model (1995), a development of the magmatic arc at the outer Gonwana margin in the form of subduction-accretion (Andean subduction type) is assumed by Tessensohn et al. (1999). The intensive partial melting combined with fast uplift may also be the consequence of an arc-continent collision with underthrusting of the continental basement as suggested by Palmeri et al. (2003) to explain the ultrahigh-pressure rocks of the Lanterman range. An underthrusting of the Bowers and Robertson Bay terranes by a microcontinent was recently discussed by Rocchi et al. (2003). A synthesis of all geological features, *i.e.* structural, metamorphic, magmatic and geochronological data to reconstruct the complicated geological evolution of the Wilson Terrane will be the subject of further work.

Due to the high closure temperature of the U-Pb isotope system in monazite (Villa, 1998), monazite ages of 494-484 Ma obtained by Schüssler et al. (1999) for samples US-380, US-495 and US-501 of the central zone were interpreted to date the high

temperature stage of metamorphism. New SHRIMP U-Pb age determinations on monazite and zircon from samples of very high-grade metamorphic rocks yielded 499±10 and 493±9 Ma for monazite and 500 ±4 Ma for one age population of metamorphic zircons (Henjes-Kunst et al., this volume). These data point to an age of about 500 Ma for the time of peak metamorphism, *i.e.* the granulite-facies stage and associated migmatisation.

The stage of isothermal decompression is followed by an increase of the cooling rate, and the P-T path reaches the stability of muscovite after crossing reaction curve (1) in a retrograde direction. A retrograde overprint under P-T conditions comparable to that in the eastern and western zones took place, leading to the formation of muscovite + biotite equilibrium assemblages in several samples. The time of this overprint may closely be dated at 476-470 Ma by Ar-Ar mica ages.

CONCLUSIONS

Compared to earlier investigations on the metamorphic basement of Oates Coast, some important new results concerning the metamorphic evolution and the exhumation history have been obtained:

(1) Until now the temporal position of the medium-pressure granulite-facies stage with P-T contitions of 8 kbar/>800°C in the central zone was questionable. A polymetamorphic evolution with a Proterozoic medium-pressure granulite-facies metamorphism and a separate Early Palaeozoic low-pressure high-grade Ross-metamorphism on the one hand and a single Ross-metamorphic evolution including the medium-pressure granulite-facies stage on the other hand were alternatively discussed (Schüssler et al., 1999). The new results show that wide areas of the central zone contain mineral assemblages indicative of medium-pressure granulite-facies stage, instead of only some small relict parts, mineral assemblages attributed to a low P/high T stage must have formed continuously as a result of decompressive reactions from medium-pressure assemblages, *e.g.* cordierite replacing garnet by reaction (6) or various amphiboles replacing orthopyroxene; these retrograde mineral reactions themselves took place under medium-pressure conditions, *i.e.* reaction (6) at >6 kbar.
A single loop metamorphic evolution during Ross Orogeny is supported by the new petrological and geochronological data.

(2) The results presented in this study show that the medium-pressure granulite-facies metamorphism also affected parts of the western zone. In contrast to the central zone, no orthopyroxene-bearing rocks could be detected in the western zone and the green spinel does also not occur in the mineral assemblages. Nevertheless, the cordierite- and garnet-forming reactions (3), (4) and (6), as observed in several samples, can clearly be attributed to this metamorphic stage. This is underscored by the P-T estimates of >6 kbar and >800°C obtained on one western zone sample. The spatial distribution of metamorphic rocks of different metamorphic grade in the western zone seems to be rather unsystematic. The lowest-grade rocks, showing that reactions (1), (2) and (3) are not overstepped or just started, are from the southern end of Burnside Ridge, Drury Nunatak and height point 740 between Rescue Nunatak and Mount Martyn. Granulite-facies rocks have been found at Rescue Nunatak, Eld Peak, and also in the region of heigh point 740. This unsystematic distribution is probably a result of internal tectonic dissection of the western zone.

(3) Ar-Ar age determinations on samples from all three zones and from the Archangel Granite, the latter having intruded low-grade metasediments of the Berg Group to the west of the western zone, demonstrate a general tendency from older to younger cooling ages from the west to the east. The amphibole ages are 488 – 486 Ma for the western zone, 485 – 481 Ma for the central zone and 472 – 469 Ma for the eastern zone. The mica ages are 484 – 482 Ma for the Archangel Granite west of the western zone, 472 Ma for the western zone, 476 – 470 Ma for the central zone and 466 Ma for the eastern zone. As shown by the amphibole ages, the cooling of the basement to the respective closure temperature in the western zone was terminated first, followed by the central and then by the eastern zone, each over a time interval of several million years. Concerning the mica data, no significant difference between the western zone and the central zone becomes obvious. If this evolution in time is correlated to exhumation, these ages may give some insight into the order of exhumation of these zones along the large thrusts, due to a compressive tectonic regime. The following scenario is likely:
First stage: the crystalline basement as a whole was thrusted along the Lazarev Thrust to the west onto the low-grade metasedimentary Berg Group rocks. During this movement, the western zone experienced the most intensive exhumation.
Second stage: the central zone was thrusted along the Exiles Thrust to the west, consequently now being strongly exhumed. A difference in time between first and second stage is documented by the ages of amphiboles which are older in the western zone as compared to the central zone. As the rather uniform mica ages in both zones indicate, the western and central zones must have experienced again a common exhumation history in the course of the late tectonometamorphic evolution.
Last stage: The eastern zone was thrusted along the Wilson Thrust to the east, onto low-grade metasedimentary rocks as can been seen at McCain Bluff.

Acknowledgements - The present paper summarizes results of investigations in the frame of the Antarctic expeditions GANOVEX V and GANOVEX VII as well as the joint German-Italian Antarctic Expedition 1999-2000. Our thanks are due to the technical and scientific participants and the crews of the expedition vessels and the helicopters who all did their very best for the success of these expeditions, and especially the expedition leaders Franz Tessensohn and Norbert Roland. Schorse Kleinschmidt, Heinz Jordan and Michael Schmidt-Thomé contributed some of their samples for our investigations, thank you for this. Thanks also to Peter Späthe (Würzburg) for the production of large amounts of thin-sections and to Klaus-Peter Kelber (Würzburg) for preparing the figures. Margot Metz and Horst Klappert are thanked for laboratory assistance during sample preparation and Ar-Ar dating at the BGR. Thanks to F. Olmi (IGG-CNR Florence) for microprobe assistance. The manuscript was critically reviewed by Simon L. Harley and Rosaria Palmeri, thank you for the substancial and helpful comments. The *Bundesanstalt für Geowissenschaften und Rohstoffe* (Hannover) and the *Deutsche Forschungsgemeinschaft* (Schu 243/9-1, Schu 873/1-1) are gratefully acknowledged for financial support. FT´s research benefitted from the support of the Italian *Programma Nazionale di Ricerche in Antartide* (project 4.2).

REFERENCES

Bhattacharya A., Mazumdar A.C. & Sen S.K., 1988. Fe-Mg mixing in cordierite: Constraints from natural data and implications for cordierite-garnet thermometry in granulites. *American Mineralogist*, **73**, 338-344.

Bohlen S.R., 1987. Pressure-temperature-time paths and a tectonic model for the evolution of granulites. *Journal of Geology*, **95**, 617-632.

Bucher K. & Frey M., 1994. *Petrogenesis of metamorphic rocks*. Springer-Verlag, Berlin-Heidelberg-New York, 318 p.

Carswell D.A. & Harley S.L., 1990. Mineral barometry and thermometry. In: Carswell, D.A. (ed.), *Eclogite facies rocks*, Blackie & Co. Publishers, London, 83-110.

Chatterjee N.D. & Johannes W., 1974. Thermal stability and standard thermodynamic properties of synthetic $2M_1$-muscovite, $KAl_2[AlSi_3O_{10}(OH)_2]$. *Contributions to Mineralogy and Petrology*, **48**, 89-114.

Dallmeyer R.D. & Wright T.O., 1992. Diachronous cleavage development in the Robertson Bay Terrane, northern Victoria Land, Antarctica: Tectonic implications. *Tectonics*, **11**, 437-448.

Di Vincenzo G., Palmeri R., Talarico F., Andriessen P.A.M. & Ricci C.A., 1997. Petrology and Geochronology of Eclogites from the Lanterman Range, Antarctica. *Journal of Petrology*, **38**, 1391-1417.

Faryad S.W. & Henjes-Kunst F., 1997. Petrological and K-Ar and ^{40}Ar-^{39}Ar age constraints for the tectonometamorphic evolution of the high-pressure Meliata unit, Western Carpathians (Slovakia). *Tectonophysics*, **280**, 141-156.

Flöttmann T. & Kleinschmidt G., 1991. Opposite thrust systems in northern Victoria Land, Antarctica: Imprints of Gondwana´s Paleozoic accretion. *Geology*, **19**, 45-47.

Flöttmann T. & Kleinschmidt G., 1993. The structure of Oates Land and Implications for the Structural Style of Northern Victoria Land, Antarctica. *Geologisches Jahrbuch*, **E 47**, 419-436.

Gibson G.M. & Wright T.O., 1985. The importance of thrust faulting in the tectonic development of northern Victoria Land, Antarctica. *Nature*, **315**, 480-483.

Grant J.A., 1985. Phase equilibria in partial melting of pelitic rocks. In: Ashworth, J.R. (ed.), *Migmatites*, Blackie & Co. Publishers, London, 86-144.

Grew E.S., Kleinschmidt G. & Schubert W., 1984. Contrasting Metamorphic Belts in North Victoria Land, Antarctica. *Geologisches Jahrbuch*, **B 60**, 253-263.

Hall A., 1987. *Igneous Petrology*. Longman Scientific and Technical, New York, 573 p.

Harley S.L., 1989. The origin of granulites: a metamorphic perspective. *Geological Magazine*, **126**, 215-247.

Harley S.L.,Thompson P., Hensen B.J. & Buick I.S., 2002. Cordierite as a sensor of fluid conditions in high-grade metamorphism and crustal anatexis. *Journal of metamorphic Geology*, **20**, 71-86.

Henjes-Kunst F. & Schüssler U., 2003. Metasedimentary units of the Cambro-Ordovician Ross Orogen in northern Victoria Land and Oates Land: geochemical and Nd-Sr isotope comparison, implications for their provenance and geotectonic consequences. *Terra Antartica*, **10**, 105-128.

Henjes-Kunst F., Roland N.W. & Dunphy J.M., 2004. SHRIMP dating of high-grade migmatites and related granitoids from the Oates Coast area (East Antarctica): evidence for a single high-grade event of Ross-orogenic age. *Terra Antartica*, this volume.

Hensen B.J. & Green D.H., 1973. Experimental Study of the Stability of Cordierite and Garnet in Pelitic Compositions at High Pressures and Temperatures. *Contributions in Mineralogy and Petrology*, **38**, 151-66.

Hensen B.J. & Harley S.L., 1990. Graphical analysis of P-T-X relations in granulite facies metapelites. In: Ashworth, J.R., Brown, M. (eds.): *High-temperature Metamorphism and Crustal Anatexis*, Unwin Hyman, London, 19-56.

Hoisch T.D., 1989. A muscovite-biotite geothermometer. *American Mineralogist*, **74**, 565-572.

Holdaway M.J. & Lee S.M., 1977. Fe-Mg Cordierite Stability in High-Grade Pelitic Rocks Based on Experimental, Theoretical, and Natural Observations. *Contributions to Mineralogy and Petrology*, **63**, 175-198.

Holdaway, M.J. & Mukhopadhyay, B., 1993. A reevaluation of the stability relations of andalusite. *American Mineralogist*, **78**, 298-315.

Holland T.J.B. & Powell, R., 1990. An enlarged and updated internally consistent thermodynamic dataset with uncertainties and correlations in the system K_2O-Na_2O-CaO-MgO-MnO-FeO-Fe_2O_3-Al_2O_3-TiO_2-SiO_2-C-H_2-O_2. *Journal of metamorphic Geology*, **8**, 89-124.

Johannes W., 1984. Beginning of melting in the granite system Qz-Or-Ab-An-H_2O. *Contributions to Mineralogy and Petrology*, **86**, 264-273.

Johannes W. & Holtz F., 1990. Formation and composition of H_2O-undersaturated granitic melts. In: Ashworth, J.R., Brown, M. (eds.), *High-temperature Metamorphism and Crustal Anatexis*, Unwin Hyman, London, 87-104.

Johannes W. & Holtz F., 1996. *Petrogenesis and Experimental Petrology of Granitic Rocks*. Springer-Verlag, Berlin-Heidelberg-New York, 335.

Kleinschmidt G. & Tessensohn, F., 1987. Early Paleozoic westward directed subduction at the Pacific margin of Antarctica. In: McKenzie, G.D. (ed.), *Gondwana Six: Structure, Tectonics, and Geophysics*, American Geophysical Union Monographs, 40, 89-105.

Kleinschmidt G., Buggisch W. & Flöttmann T., 1992. Compressional causes for the Early Paleozoic Ross Orogen - evidence from Victoria Land and the Shackleton Range. In: Yoshida, Y. et al. (eds.), *Recent Progress in Antarctic Earth Science*, Terra Scientific Publication Company, Tokyo, 227-233.

Le Fort P., 1981. Manaslu leucogranite: a collision signature of the Himalaya, a model for its genesis and emplacement. *Journal of Geophysical Research*, **86**, 10545-10568.

Lee H.Y. & Ganguly J., 1988. Equilibrium compositions of coexisting garnet and orthopyroxene: experimental determinations in the system FeO-MgO-Al_2O_3-SiO_2, and applications. *Journal of Petrology*, **29**, 93-113.

Loomis, T.P., 1976. Irreversible reactions in high-grade metapelitic rocks. *Journal of Petrology*, **17**, 559-588.

Martignole J. & Sisi J.-C., 1981. Cordierite-Garnet-H_2O Equilibrium: A Geological Thermometer, Barometer and Water

Fugacity Indicator. *Contributions to Mineralogy and Petrology*, **77**, 38-46.

Massonne H.-J. & Schreyer W., 1987. Phengite geobarometry based on the limiting assemblage with K-feldspar, phlogopite, and quartz. *Contributions to Mineralogy and Petrology*, **96**, 212-224.

Matzer S., 1995. Paläozoische Akkretion am paläopazifischen Kontinentalrand der Antarktis in Nordvictorialand - P-T-D-Geschichte und Deformationsmechanismen im Bowers Terrane. *Berichte zur Polarforschung*, **173**, 1-234.

Mehnert K.R., 1968: *Migmatites and the origin of granite rocks*. Elsevier, Amsterdam, 393 p.

Palmeri R., 1997. P-T paths and migmatite formation: An example from Deep Freeze Range, northern Victoria Land, Antarctica. *Lithos*, **42**, 47-66.

Palmeri R., Ghiribelli B., Talarico F. & Ricci C.A., 2003. Ultra-high-pressure metamorphism in felsic rocks: the garnet-phengite gneisses and quartzites from the Lanterman Range, Antarctica. *European Journal of Mineralogy*, **15**, 513-526.

Powell R. & Holland T.J.B., 1994. Optimal geothermometry and geobarometry. *American Mineralogist*, **79**, 120-133.

Rocchi S., Tonarini S., Armienti P., Innocenti F. & Manetti P., 1998. Geochemical and isotopic structure of the early Palaeozoic active margin of Gondwana in northern Victoria Land, Antarctica. *Tectonophysics*, **284**, 261-281.

Rocchi S., Capponi G., Crispini L., Di Vincenzo G., Ghezzo C., Meccheri M. & Palmeri R., 2003. Mafic rocks at the Wilson-Bowers terrane boundary and within the Bowers Terrane: clues to the Ross geodynamics in northern Victoria Land, Antarctica. *9th International Symposium of Antarctic Earth Sciences, 8.-12.9.2003, Potsdam, abstracts*, 275-276.

Roland, N.W., Adams, C.J., Flöttmann, T., Kleinschmidt, G., Olesch, M., Schüssler, U., Skinner, D.N.B. & Wörner, G., 1996. Geological map of the Suvorov Glacier quadrangle, Victoria Land, Antarctica, 1:250.000. *GIGAMAP*, Bundesanstalt für Geowissenschaften und Rohstoffe, Hannover.

Roland N.W., Henjes-Kunst F., Kleinschmidt G. & Talarico F., 2000. Petrographical, geochemical and radiometric investigations in Northern Victoria Land, Oates Land and George V Coast: towards a better understanding of plate boundary processes in Antarctica. *Terra Antartica Reports*, **5**, 57-65.

Roland N.W., Adams C.J., Flöttmann T., Kleinschmidt G., Olesch M., Pertusati P.C., Schüssler U., Skinner D.N.B. & Henjes-Kunst F., 2001. Geological map of the Matusevich Glacier quadrangle, Victoria Land, Antarctica, 1:250.000. *GIGAMAP*, Bundesanstalt für Geowissenschaften und Rohstoffe, Hannover.

Schubert, W. & Olesch, M., 1989. The Petrological Evolution of the Crystalline Basement of Terra Nova Bay, North Victoria Land, Antarctica. *Geologisches Jahrbuch* , **E 38**, 277-298.

Schüssler U., 1996. Metamorphic rocks in the Northern Wilson Terrane, Oates Coast, Antarctica. *Geologisches Jahrbuch*, **B 89**, 247-269.

Schüssler U. & Henjes-Kunst F., 1994. Petrographical and geochronological investigations on a garnet-tourmaline pegmatite from Ringgold Knoll, Oates Coast, Antarctica. *Chemie der Erde*, **54**, 297-318.

Schüssler U., Fenn, G., Flöttmann T., Kleinschmidt G., Olesch M., Roland N., Schubert W. & Skinner D.N.B., 1998. Geological map of the Pomerantz Tableland quadrangle, Victoria Land, Antarctica,1:250.000. *GIGAMAP*, Bundesanstalt für Geowissenschaften und Rohstoffe, Hannover.

Schüssler U., Bröcker M., Henjes-Kunst F. & Will T., 1999. P-T-t evolution of the Wilson Terrane metamorphic basement at Oates Coast, Antarctica. *Precambrian Research*, **93**, 235-258.

Spear F.S., 1993. *Metamorphic Phase Equilibria and Pressure-Temperature-Time-Paths*. Mineralogical Society of America Monograph, Washington D.C., 799 p.

Steiger R.H. & Jäger E., 1977. Subcommission on geochronology. Convention on the use of decay constants in geo- and cosmochronology. *Earth and Planetary Science Letters*, **36**, 359-362.

Talarico F., 1990. Reaction textures and metamorphic evolution of aluminous garnet granulites from the Wilson Terrane (Deep Freeze Range, North Victoria Land, Antarctica). *Memorie della Società Geologica Italiana*, **43**, 49-58.

Talarico F. & Castelli D., 1994. Migmatitic Metasedimentary Granulites from Mills Peak and Mt. Emison (Wilson Terrane, Northern Victoria Land, Antarctica): A Case History of Processes involved in the Formation of Garnet ± Orthopyroxene Leucocratic Segregations. *Terra Antartica*, **1**, 19-22.

Talarico F. & Castelli D., 1995. Relict granulites in the Ross orogen of northern Victoria Land (Antarctica), I. Field occurrence, petrography and metamorphic evolution. *Precambrian Research*, **75**, 141-156.

Talarico F., Memmi I., Lombardo B. & Ricci C.A., 1989. Thermobarometry of granulite rocks from the Deep Freeze Range, North Victoria Land, Antarctica. *Memorie della Società Geologica Italiana*, **33**, 131-142

Talarico F., Borsi L. & Lombardo B., 1995. Relict granulites in the Ross orogen of northern Victoria Land (Antarctica), II. Geochemistry and paleo-tectonic implications. *Precambrian Research*, **75**, 157-174.

Tessensohn F., Kleinschmidt G., Talarico F., Buggisch W., Brommer A., Henjes-Kunst F., Kroner U., Millar I.L. & Zeh A.,1999. Ross-Age Amalgamation of East and West Gondwana: Evidence from the Shackleton Range, Antarctica. *Terra Antartica*, **6**, 317-325.

Thompson A.B. & England P.C., 1984. Pressure-Temperature-Time Paths of Regional Metamorphism II. Their Inference and Interpretation using Mineral Assemblages in Metamorphic Rocks. *Journal of Petrology*, **25**, 929-955.

Villa I.M., 1998. Isotopic closure. *Terra Nova*, **10**, 42-47.

Weaver S.D., Bradshaw J.D. & Laird M.G., 1984. Geochemistry of Cambrian volcanics of the Bowers Supergroup and implications for the Early Palaeozoic tectonic evolution of northern Victoria Land, Antarctica. *Earth and Planetary Science Letters*, **68**, 128-140.

Wilson, M. (1989): *Igneous Petrogenesis*. Unwin Hyman, London, 466 p.

Xu G., Will T.M. & Powell R., 1994. A calculated petrogenetic grid for the system K_2O-FeO-MgO-Al_2O_3-SiO_2-H_2O, with particular reference to contact-metamorphosed pelites. *Journal of metamorphic Geology*, **12**, 99-119.

Appendix - Analytical methods.

Mineral analysis on samples from GANOVEX V and VII (Tab. 2a) were done at the Institute of Mineralogy, University Würzburg, using a CAMECA SX50 electron microprobe with 4 wavelength-dispersive spectrometers. Operating conditions were 15 kV accelerating voltage and 15 nA beam current. Counting time was 20 s for each, peak and background, except for Fe, Mn and Zn (30 s). Natural and synthetic silicates and oxides were used as reference standards. Matrix correction was calculated by the PAP program from CAMECA. The analytical error is <1% relative for major elements except Na (<2%). The detection limit is between 0.05 and 0.1 wt.%. Measurements on samples from the joint German-Italian Antarctic Expedition 1999-2000 (Tab. 2b) were carried out at the *Istituto di Geoscienze e Georisorse* (CNR) in Florence, using a JEOL JX 8600 electron microprobe fitted with four wavelength-dispersive spetrometers. Accelerating voltage was 15 kV and the sample current was 10 nA. Natural standards were used for calibration.

Ar-Ar analyses were carried out at the BGR Hannover following the method described in Faryad & Henjes-Kunst (1997). Hand-picked concentrates with sample weights of approximately 4 - 170 mg, depending on potassium concentration and the amount of sample material available were dated. Gas was extracted during up to 19 heating steps, each step retaining a constant temperature for 30 min, up to a maximum temperature of 1550°C to ensure total degassing of the samples. Measured isotopic ratios were corrected for mass discrimination, total-system blank, decay of ^{39}Ar and ^{37}Ar, and for interfering isotopes. The error in the $^{40}Ar/^{39}Ar$ step ages was calculated by error propagation of uncertainties including those of the in-run statistical parameters and the errors derived from the blank contributions, and the correction factors. The total-gas, integrated and plateau ages also take into account the uncertainty in the flux calibration. All errors are given at the 95% confidence level. The ages were calculated using the IUGS-recommended constants (Steiger & Jäger 1977).